DMD Fast Forward. Published on July 4, 2020 as DOI: 10.1124/dmd.120.000013
This article has not been copyedited and formatted. The final version may differ from this version.

Title Page

Simplifying the Execution of HepatoPac MetID Experiments: Metabolite Profile and Intrinsic Clearance Comparisons

T. Eric Ballard, N. Kratochwil, Loretta M. Cox, Mark A. Moen F. Klammers, A. Ekiciler, A. Goetschi and I. Walter

Global Drug Metabolism and Pharmacokinetics, Takeda Pharmaceuticals Co., Cambridge, MA 02139, USA; TEB (Current)

Pharmacokinetics, Dynamics and Metabolism, Pfizer, Inc., Groton, CT 06340, USA; TEB, LMC, MAM

Drug Disposition and Safety, Roche Pharmaceutical Research and Early Development, Roche Innovation Center, 4070 Basel CH, Switzerland; NK, FK, AE, AG, IW

DMD Fast Forward. Published on July 4, 2020 as DOI: 10.1124/dmd.120.000013
This article has not been copyedited and formatted. The final version may differ from this version.

Running Title Page

Running Title: Simplified Execution of HepatoPac® for MetID

Corresponding Author:

T. Eric Ballard

Global Drug Metabolism and Pharmacokinetics, Takeda Pharmaceuticals Co., Cambridge, MA 02139, USA

(Tel) +1 (617) 551-3682; eric.ballard@takeda.com

Document Statistics:

Text Pages: 12

Tables: 1

Figures: 6

References: 22

Abstract: 160 words (200 max)

Introduction: 557 words (750 max)

Results and Discussion: 1325 words (1500 max)

Keywords:

Biotransformation, micropatterned co-culture, HepatoPac®, metabolite ID, intrinsic clearance and low clearance

Abbreviations:

ADME: absorption, distribution, metabolism and excretion; AKR: aldo-keto reductase; AO: aldehyde oxidase; BG: background; CYP: cytochrome P540; DME: drug metabolizing enzyme; DMSO: dimethylsulfoxide; FMO: flavin-containing monooxygenase; Cl_{int}: Intrinsic Clearance; LCMS: liquid chromatography mass spectrometry; LC-MS/MS: liquid chromatography with tandem mass spectrometry; MPCC: micropatterned co-culture; MS: mass spectrometry; NAT: *N*-acetyltransferase; PAL: prep and

DMD Fast Forward. Published on July 4, 2020 as DOI: 10.1124/dmd.120.000013
This article has not been copyedited and formatted. The final version may differ from this version.

load; RSE%: Relative Standard Error; SULT: sulfotransferase; UGT: urinidine 5'-diphospho-glucuronosyltransferase; UHPLC: ultra-high pressure liquid chromatography; UV: ultraviolet; XIC: extracted ion chromatogram

DMD Fast Forward. Published on July 4, 2020 as DOI: 10.1124/dmd.120.000013
This article has not been copyedited and formatted. The final version may differ from this version.

Abstract

The HepatoPac® micropatterned co-culture (MPCC) hepatocyte system has been shown to be an effective tool to investigate the qualitative human and preclinical species' metabolite profiles of new drug candidates. However, additional improvements to the overall study conditions and execution, layout and human donor count could be made. To that end, we have evaluated several ways to increase the amount of data one can generate per MPCC plate and how to more efficiently execute a MPCC study for the purpose of metabolite generation. Herein, we compared a set of compounds using single and 10-donor pooled human MPCC hepatocytes. Intrinsic Clearance (Cl_{int}) and mean metabolic activities assessed by diverse enzyme markers was comparable between the single and 10-donor pool. We have confirmed that the generated metabolite profiles were indistinguishable between the single and 10-donor pool, and also that rat MPCC can be performed at 400 µL media volume which greatly simplifies study execution. Additional tips for successful study execution are also described.

Significance Statement

When using the HepatoPac® MPCC system, sometimes simple experimental condition variables or problematic plate designs could hamper productive study execution. We evaluated conditions to increase the amount of data one can generate per MPCC plate and, perhaps more importantly, execute that study more efficiently with less likelihood of error. We describe some of our key learnings, provide an examination of enzyme activity levels and clearance values, and provide some recommendations to simplify the execution of a HepatoPac® experiment.

Introduction

Intrinsic clearance estimates and biotransformation studies of small molecules is an essential part of the drug discovery process (Plant, 2004; Pelkonen and Raunio, 2005; Kerns, 2008). In the previous decades, liver preparations of microsomes, cytosol, S9 fraction and, later, cryopreserved suspended hepatocytes proved amply useful at providing actionable metabolism information to progress programs forward (Plant, 2004; Pelkonen and Raunio, 2005; Dalvie et al., 2009). Chemists have become increasingly skilled at designing small molecules that are more metabolically stable, driving clearance

DMD Fast Forward. Published on July 4, 2020 as DOI: 10.1124/dmd.120.000013
This article has not been copyedited and formatted. The final version may differ from this version.

values ever lower. Very low clearance compounds make the accurate measurement of intrinsic clearance and biotransformation studies increasing difficult (Kerns, 2008; Di and Obach, 2015; Hutzler et al., 2015). Over the past several years, several methods and products have risen to meet this challenge by prolonging the exposure of compounds (and their metabolites) to fresh hepatocytes through a relay or extending the stability of hepatocytes allowing compounds to be incubated for many days and weeks without significant loss of enzyme activity (Khetani and Bhatia, 2008; Dash et al., 2009; Wang et al., 2010; Chan et al., 2013; Ballard et al., 2014; Ballard et al., 2016; Bonn et al., 2016; Hultman et al., 2016; Burton et al., 2018).

In this study, we sought to investigate a few important questions regarding the HepatoPac® system and to provide some clarity on the execution of metabolite ID studies in the HepatoPac® system through the sharing of some of our solutions to problems we have encountered. We specifically sought to 1) compare the effect of media volume on metabolite profiles in rat MPCC hepatocytes and 2) compare metabolite profiles and intrinsic clearance values of single donor micropatterned co-cultured (MPCC) hepatocytes to a 10-donor pool of human MPCC hepatocytes. We sought to use a 10-donor pool to maximize the available incubations per plate/experiment, investigate future opportunities to create higher overall enzyme activity pools and protect against single donor inter-individual variability in the HepatoPac® system. For scientists working with rat MPCC and the multi-species HepatoPac® plates, it is a common frustration to have to treat the rat MPCC hepatocyte wells differently than all the other species (recommended rat media volume is 300 µL vs 400 µL for all other species) which can lead to complicated dosing and sampling regimes. So, to simplify experimental execution we were interested in testing whether or not the media volume differences for rat MPCC hepatocytes resulted in any detectable differences in the metabolite profiles of our test compounds (Figure 1). The test set was chosen to represent moderate to low clearance compounds with single and complex/multi-step metabolic pathways across several enzyme classes, as well as, to complement our previous research with these compounds (Ballard et al., 2016).

The multispecies MPCC plate design could also be further simplified and made to accommodate a greater variety of species or testable experimental conditions if the three individual human donor columns were eliminated in favor of a 10-donor human MPCC hepatocyte pool. A benefit of consolidating the

DMD Fast Forward. Published on July 4, 2020 as DOI: 10.1124/dmd.120.000013
This article has not been copyedited and formatted. The final version may differ from this version.

three individual human donors into one column is that this would then allow for the fibroblast controls to be included on the same plate. To that end, we examined the intrinsic clearances of our set of test compounds in both single and 10-donor MPCCs and also determined the enzyme activity levels of the single and 10-donor MPCC systems using probe substrates for 13 common drug metabolizing enzymes (DMEs).

Materials and Methods

Materials. Carbazeran and quinidine were obtained from Pfizer Global Material Management (Groton, CT). Sunitinib was purchased from AK Scientific (Union City, CA). Tolbutamide and trifluoperazine were purchased from Sigma Aldrich (St. Louis, MO). MPCC hepatocyte 24-well plates containing human donor VNL (female), pooled 10-donor human YFA (mixed gender), rat donor and mouse fibroblast controls were provided by Ascendance Biotechnology (Medford, MA – now BioIVT, Westbury, NY). The MPCCs were purchased from Ascendance Biotechnology and treated as previously described prior to shipment (Ballard et al., 2016). For performing biotransformation metabolite ID experiments, MPCC hepatocytes were plated in a 1:3 ratio of fibroblasts:hepatocytes (with ~25K hepatocytes/well) in a 24-well plate. 96-well plates containing MPCC hepatocytes in a 1:3 ratio with 3200 hepatocytes/well were used for intrinsic clearance experiments (donor specification sheets provided by the supplier). A total hepatocyte protein content of 0.005 mg mL^{-1} (0.0032 mg per well) was therefore applied for the 96-well HepatoPac® format as described previously (Kratochwil et al., 2017). Fibroblast controls were included on the same plate for the biotransformation metabolite ID experiments (mouse and human) while separate fibroblast control plates were used for the intrinsic clearance experiments (mouse only). Unless stated otherwise, all other solvents and compounds were purchased from ThermoFisher Scientific (Waltham, MA).

Biotransformation Metabolite ID Using MPCC Hepatocyte Plates. Studies were adapted from previously described methods (Ballard et al., 2016). Briefly, 24-Well MPCC plates were shipped to Pfizer, fresh medium was applied and cultures were kept at 37 °C with 90% O_2/10% CO_2 and 95% relative humidity for two days. MPCCs were changed to serum-free medium 2 h prior to compound treatment. The MPCC hepatocytes (and on plate fibroblast controls) were incubated with test compounds (37 °C with 90% O_2/10% CO_2 and 95% relative humidity) at a final concentration of 10 µM (chosen to provide

DMD Fast Forward. Published on July 4, 2020 as DOI: 10.1124/dmd.120.000013
This article has not been copyedited and formatted. The final version may differ from this version.

quality ultraviolet (UV) and mass spectrometry (MS) data) in treatment media (dimethylsulfoxide (DMSO) final concentration ≈ 0.03%) with a final volume of 400 µL (with the exception of rat hepatocytes at 300 µL for the comparison study). At 0, 48 and 168 h, the culture medium was removed from respective wells and transferred to 15 mL vials. Time zero samples were supernatant only based on the sampling protocol and proteins were precipitated with 1600 uL of acetonitrile. For the 48 and 168 h time points, the wells were transferred to 15 mL vials then the wells were washed with 2 x 800 µL of acetonitrile (scraping the bottom of the wells with the pipet tips to detach cells) and the washes were pooled with the corresponding precipitated samples. The samples were mixed on a vortex mixer, centrifuged (1280 x *g*, 5 min) and the supernatants transferred to new 15 mL conical glass tubes. The supernatants were dried in a Genevac™ (Genevac Inc, Valley Cottage, NY) evaporative centrifuge and the resulting residues were reconstituted in 100 µL of 95% water (0.15% formic acid) / 5% acetonitrile (300 µL rat time point samples were reconstituted into 75 µL with same 95%/5% proportions to normalize the resuspension concentrations), centrifuged (1280 x *g*, 5 min) and analyzed by liquid chromatography mass spectrometry (LCMS). All compounds were incubated in the MPCC hepatocytes with the same time point collections, regardless of known or expected clearance rates (human or rat), based on previous studies in HepatoPac® and hepatocyte relay systems (Ballard et al., 2014; Ballard et al., 2016). For a more detailed description on the execution of the biotransformation metabolite ID study, please see the expanded section (vide infra).

Ultra-High Pressure Liquid Chromatography (UHPLC)-Tandem Mass Spectrometry Analysis for Metabolite ID Profiling. Mass Spectrometric conditions were adapted from previously described methods (Ballard et al., 2016). Briefly, reconstituted samples were analyzed by UHPLC-UV-MS operated in positive or negative ion mode (negative mode only used for detection of tolbutamide *N*-dealkylation product) using an Orbitrap Elite mass spectrometer. For UHPLC-UV-MS analysis, the capillary temperature was set at 275 °C, the source potential was 3500 V (used same source potential for both positive and negative mode scanning) and the source heater was set at 425 °C. The mass spectrometer was operated in a data-dependent scanning mode to MS^3 with dynamic exclusion enabled (repeat count: 1; repeat duration: 5.0 s; list size: 500; exclusion duration: 1.5 s). The normalized collision energy for the data-dependent scans was 35%. Other potentials were adjusted as necessary to get optimal ionization

DMD Fast Forward. Published on July 4, 2020 as DOI: 10.1124/dmd.120.000013
This article has not been copyedited and formatted. The final version may differ from this version.

and fragmentation of the parent compound. UV absorption spectra were obtained by an in-line Accela photodiode array detector. A Kinetex EVO C18 100 Å column (2.1 × 150 mm, 1.7 µm; Phenomenex, Torrance, CA) was used with a flow rate of 0.4 mL/min at 45 °C (except for quinidine: flow rate of 0.3 mL/min). Mobile phase A was comprised of 0.1% formic acid and mobile phase B was comprised of acetonitrile. For carbazeran, sunitinib and tolbutamide, the gradient system used was: initially, 5% B held for 0.8 min followed by a linear gradient to 50% B from 0.8 to 8.25 min, a second linear gradient to 95% B at 8.5 to 8.75 min, a 0.25 min wash at 95% B, a third linear gradient to 5% B at 9 to 9.2 min and finally a 0.8 min reequilibration period at 5% B. For trifluoperazine, the gradient system used was: initially, 5% B held for 0.8 min followed by a linear gradient to 95% B from 0.8 to 8.25 min, a 0.75 min wash at 95% B, a third linear gradient to 5% B at 9 to 9.2 min and finally a 0.8 min reequilibration period at 5% B. For quinidine, the flow rate was 0.3 mL/min and the gradient system used was: initially, 5% B held for 0.8 min followed by a linear gradient to 40% B from 0.8 to 8.25 min, a second linear gradient to 95% B at 8.5 to 8.75 min, a 0.25 min wash at 95% B, a third linear gradient to 5% B at 9 to 9.2 min and finally a 0.8 min reequilibration period at 5% B. Injections of 10 µL were made by a CTC Prep and Load (PAL) autosampler (CTC Analytics, Zwingen, Switzerland).

Intrinsic Clearance Determinations and Metabolic Activity Profiling. Studies were adapted from previously described methods (Kratochwil et al., 2017). Briefly, after a recovery of 48 h at 37 °C and 10% CO_2, the HepatoPac® plates were washed once with application medium (64 µL serum-free Dulbecco's modified Eagle's medium specially formulated for HepatoPac® cultures) and then a fresh media (64 µL) was pre-incubated for 2 h at 37 °C and 10% CO_2 before adding the compounds. For clearance determinations, quinidine, sunitinib, tolbutamide were tested at a concentration of 1 µM and trifluoperazine at a concentration of 0.3 µM and carbazeran at concentrations of 0.3, 1 and 3 µM, respectively [Footnote 1]. For metabolic activity determination, the following enzyme substrates were added to HepatoPac® plates and incubated at 5% CO_2 atmosphere and at 37 °C: Benzydamine [flavin-containing monooxygenase (FMO)] at 1 µM ; midazolam [cytochrome P450 (CYP)3A4], and dextromethorphan (CYP2D6) at 5 µM; 7-hydroxycoumarin [sulfotransferase (SULT) and urinidine 5'-diphospho-glucuronosyltransferase (UGT)] diclofenac (CYP2C9), tacrine (CYP1A2), daunorubicin [aldo-keto reductase (AKR)] and O_6-benzyl guanine [aldehyde oxidase (AO)] at 10 µM; bupropion (CYP2B6),

DMD Fast Forward. Published on July 4, 2020 as DOI: 10.1124/dmd.120.000013
This article has not been copyedited and formatted. The final version may differ from this version.

amodiaquine (CYP2C8) and sulfamethazine [*N*-acetyltransferase (NAT)] at 20 µM, and SN-38 (UGT1A1) at 50 µM, respectively. The final DMSO content in the medium was 0.1% DMSO. At defined time points, samples were drawn and quenched with acetonitrile (volume ratio 1:2) containing an internal standard (oxazepam). Samples were then cooled, centrifuged (6000 x *g*, 10 min) and quantified by using liquid chromatography with tandem mass spectrometry (LC-MS/MS).

HPLC-Mass Spectrometry Analysis for Intrinsic Clearance and Metabolic Activity. Mass spectrometric conditions were adapted from previously described methods (Kratochwil et al., 2017). Briefly, LC-MS/MS was used for the quantification of the compounds. The HPLC system consisted of 30AD Shimadzu pumps. The analytical columns used were a Phenomenex Synergi Polar-RP C18 (5 cm × 1 mm; 3.5 µm) for 7-hydroxycoumarin and a Supelco Ascentis Express C18 (2 cm × 2.1 mm; 2.7 µm) at 60 °C for the other analytes. A Q6500+ Sciex mass spectrometer equipped with a TurboIonSpray source (IonSpray Voltage 5500V in positive mode, -4500V in negative mode) and a HTS CTC PAL autosampler were used. Mobile phase A was 0.5% formic acid in water:methanol 95:5, mobile phase B was acetonitrile. Aliquots (1 µL) of the diluted sample solutions were injected and transferred to the analytical column at a flow rate of 600 µL/min. To elute the compounds, a high-pressure linear gradient from 0% to 95% B in 40 seconds was applied. Total run time was 1.6 min.

Data Analysis for Intrinsic Clearance and Metabolic Activity. Data were analyzed as previously using quadratic regression with $1/x^2$ weighting on peak area ratios (Kratochwil et al., 2017). The precision and accuracy of the standard and QC samples were between 80 and 120%. Analyst software (Version 1.6.2, Sciex, Framingham, USA) was employed for data processing. For determination of the intrinsic clearance, pharmacokinetic modeling was applied in the Monolix® software (Version 4.33, Lixoft – Incuballiance, Orsay, France) by using a nonlinear mixed-effects approach to in vitro single time–concentration profiles. The statistical unit was the well and inter-well variability on the derived parameters was explored. The details for the intrinsic clearance determination are described elsewhere (Kratochwil et al., 2017). To calculate the metabolic rates, a linear fit was made to the determined concentrations of the metabolites plotted against time. The linear rate was then normalized by the protein content of the cells to derive at the metabolite formation rate (pmol min^{-1} mg^{-1} protein). To derive at the metabolic activity index (µL min^{-1} mg^{-1} protein), the derived metabolite formation rates were further divided by the

DMD Fast Forward. Published on July 4, 2020 as DOI: 10.1124/dmd.120.000013
This article has not been copyedited and formatted. The final version may differ from this version.

substrate concentration used in the incubation (Supplemental Table 2). Intrinsic clearance values and metabolic rates were also determined in mouse embryonic 3T3 fibroblast only control plates and the derived intrinsic clearance and metabolic rates corrected as described previously (Kratochwil et al., 2017) (Supplemental Table 3).

Expanded Biotransformation Metabolite ID Protocol. For comparison of the single human VNL donor and the 10-donor pooled MPCC hepatocytes, two 24-well plates were used with the first plate containing the single human donor MPCC and the second containing the 10-donor pooled MPCC hepatocytes. Plates were divided in half with the MPCC on one side and the stromal only controls on the other (Supplemental Excel File - Plate Map). Columns one and six were used as control wells and test compounds were dosed in columns two through five. Rows one and four were used for the time zero / day 2 samples while rows two and three were used for day 7 samples. By having the earliest time points and controls located on the outside wells, loss of volume due to evaporation in the later time points was mitigated (despite 95% humidity, evaporation was still noticeable after seven days).

To streamline compound and sample manipulation, a dosing plate was prepared containing 2X concentrations of test compounds in media. With a variety of compounds being tested on multiple plates, implementing a dosing plate in the same format as the test plates allowed for a smoother workflow and reduced the chance of sample handling error. After 2 h incubation with the serum-free media, the media was removed and then half of the media volume (200 µL) was added to the wells prior to dosing with test compound. 168 h wells were then dosed first from the dosing plate followed by the 0/48 h wells. Supernatant samples were removed immediately from the day 0/2 wells and transferred to conical tubes containing 4X volumes of acetonitrile. Media (200 µL) was then immediately added back to the 0/48 h wells and then re-dosed with test compound from the dosing plate to be used as the 48 h samples. 48 and 168 h time points were sampled by removing the entire supernatant volume of the respective wells and transferring to conical vials. Acetonitrile (2X volume) was then added to the wells and the bottom of the plates exfoliated with pipet tips. The resulting suspensions were then pooled with the corresponding supernatants. Wells were washed a second time with acetonitrile (2X volume) and pooled with the corresponding suspensions. When taking the 48 h time point, blank media was added back to the sampled wells to maintain humidity levels in the plate.

DMD Fast Forward. Published on July 4, 2020 as DOI: 10.1124/dmd.120.000013
This article has not been copyedited and formatted. The final version may differ from this version.

Wells containing rat hepatocytes were treated similarly as described above. Wells only containing 300 µL of media were prepared in the same manner as wells with 400 µL of media except after dosing the plate 100 µL of sample was removed from each rat hepatocyte well and discarded (leaving 300 µL). The human MPCC time point sampling protocol outlined above was used for the rat MPCC studies.

Results

Rat Media Volume Assessment:

The test set of compounds were incubated at 10 µM in rat MPCC hepatocytes for 168 h taking zero, 48 and 168 h time points, respectively. Using the 168 h time point as representative, metabolite ID profiles for each compound were compared and were indistinguishable when run at the recommended 300 µL volume vs the desired 400 µL volume (Figure 2 and 3; Supplemental Figures 1-9).

Single Human Donor VNL vs. 10-Donor Pool MPCC Assessment of MetID Profile and Clearance Rates:

The test set of compounds were incubated at 10 µM in single and 10-donor pooled human MPCC hepatocytes for 168 h taking zero, 48 and 168 h time points, respectively. The 10-donor pool was prepared by BioIVT independent of this investigation and so the VNL single donor was not specifically included as one of the donors within the pool. The VNL donor was used in this investigation from previous experience (Ballard et al., 2016) and there was no specific selection criteria imposed beyond VNL representing average metabolic activity. Using the 168 h time point as representative, metabolite ID profiles for each compound were compared and were indistinguishable between the single and 10-donor incubations (Figure 4; Supplemental Figures 11-14). Intrinsic Clearance values were determined at 1 µM (trifluoperazine 0.3 µM and carbazeran 0.3 – 3 µM) with time points taken up to 96 h (Table 1; Supplemental Figure 10 and Supplemental Table 4). Similar Cl_{int} values were obtained for quinidine, sunitinib, trifluoperazine and carbazeran while tolbutamide displayed a 2.7-fold lower clearance value in the 10-donor pool.

Metabolic Activity Assessment of Single Human Donor VNL vs 10-Donor Pool MPCC:

DMD Fast Forward. Published on July 4, 2020 as DOI: 10.1124/dmd.120.000013
This article has not been copyedited and formatted. The final version may differ from this version.

Thirteen diverse phase I and phase II enzyme markers were used to compare metabolic activity of the single vs 10-donor MPCC hepatocytes. In general, similar mean metabolic activities were found for the single VNL donor and the 10-donor pool with average metabolic activity index values of 58 and 37, respectively. The single VNL donor displays an average 1.6-fold higher activity across of the enzyme marker studied (Figure 5; Supplemental Table 1). Notable differences were NAT with 3-fold higher activity in the single donor while CYP2B6 was >10-fold lower in the single donor.

Discussion

Our overall goal in this investigation was to streamline the execution of a biotransformation metabolite identification experiment using a multi-species MPCC HepatoPac® plate and confirm that a 10-donor human MPCC HepatoPac® plate was equivalent or better than a single donor for both metabolite identification and intrinsic clearance determinations. We sought to use a 10-donor pool to maximize the available incubations per plate/experiment and protect against single donor inter-individual variability in the HepatoPac® system. Our first evaluation began with assessing the effects of incubations volumes on the rat MPCC hepatocyte metabolite profiles with a test set of compounds. The compounds were incubated at 10 µM final concentration in either 300 or 400 µL media volume and samples were removed for analysis at initiation of the experiment (T = 0 h) and at 48 and 168 h of incubation at 37 °C. Regardless of time point, metabolite profiles for the test set of compounds at the recommended 300 µL media volume for rat MPCC hepatocytes were indistinguishable from the 400 µL incubations (Figure 2; Supplemental Figures 1-8). This result, although on a limited test set, provides evidence that the rat and the multi-species MPCC (that includes rat MPCC) HepatoPac® plate can be simplified to use 400 µL of media volume across the entire plate greatly decreasing the chance for dosing error and providing an easier execution of the experiment. Carbazeran, as a representative example, displayed an equal production of metabolites resulting from multiple metabolic pathways: oxidative demethylation (*m/z* 333 and 347), AO (*m/z* 377), direct conjugations (*m/z* 523b and *m/z* 537) and secondary metabolites (*m/z* 349, 427 and 523a) (Figure 2 and 3). Tolbutamide metabolism in rat forms a urea dealkylation metabolite that is not formed in human and the formation of this metabolite was also unaffected by the incubation media volume (Supplemental Figure 9) (Gee et al., 1984; Back and Orme, 1989). Clearance rates of the

DMD Fast Forward. Published on July 4, 2020 as DOI: 10.1124/dmd.120.000013
This article has not been copyedited and formatted. The final version may differ from this version.

test compounds were not assessed in rat MPCC hepatocytes at either volume. No metabolism was detected for any of the test compounds in mouse fibroblast co-culture cells at either volume tested (Figure 2 and Supplemental Figures 1-4).

Following our evaluation of the rat media volume we sought to assess the ability to simplify the HepatoPac® plate design by using a 10-donor human pool vs using three separate donors on a single plate. Throughout discovery absorption, distribution, metabolism and excretion (ADME) scientific investigations, donor pools are used for nearly all preclinical and human (usually a pool of 10+ mixed-gender) liver subcellular fractions (especially hepatocytes) in an effort to maximize enzymatic activity and protect against inter-individual variability. A follow-on output of this research was to provide evidence that a platable pool of 10 donors could, potentially, be used in place of the three individual hepatocyte donors. Generating a pool of platable hepatocytes and ensuring that all hepatocyte donors are ~equally represented in the MPCC is not a simple task and is still actively under investigation. However, the activity of the 10 individual donors was assessed in suspension across a number of enzymes and their mean activity was in agreement with the activity of the pooled hepatocyte MPCCs suggesting equivalent representation of each donor (Heyward et al., 2016).

To evaluate the metabolite profile differences that may arise, the set of compounds were incubated at 10 µM in single VNL and 10-donor MPCC hepatocytes for 168 h taking time points at zero, 48 and 168 h. In parallel experiments, Cl_{int} was also measured for each compound over the course of several hours to days (depending on the rate of clearance) in both the single and 10-donor MPCC hepatocytes.

As a whole, Cl_{int} for the set of compounds was comparable between the single and 10-donor MPCC hepatocyte incubations. Cl_{int} values (µL/min/mg protein) for quinidine, sunitinib, trifluoperazine and carbazeran were similar between the single and 10-donor pool (Table 1) which also provides evidence that UGT1A1 (trifluoperazine), CYP3A (quinidine and sunitinib) and AO (carbazeran) have equivalent activities between the two systems (further evaluated below). Tolbutamide, a CYP2C9 substrate, displayed a 2.7-fold higher clearance in the single donor MPCC, which can be attributed to donor variability (Lombardo et al., 2013; Jones, 2015). Although the clearance for tolbutamide was higher in the single donor MPCC, the metabolite profile was indistinguishable between the single and 10-donor MPCC

DMD Fast Forward. Published on July 4, 2020 as DOI: 10.1124/dmd.120.000013
This article has not been copyedited and formatted. The final version may differ from this version.

human hepatocytes (Figure 4 and Supplemental Figure 11). To that end, the metabolite profiles for quinidine, sunitinib and trifluoperazine, carbazeran and tolbutamide in the single and 10-donor MPCC hepatocytes were qualitatively indistinguishable from each other at all time points (Supplemental Figures 12-14).

As a follow-up to the Cl_{int} and metabolite profile assessments of our test set of compounds, we also investigated the enzymatic activity of the single and 10-donor MPCC hepatocytes using 13 diverse enzyme markers. Metabolite formation was measured in both systems for up to 6 h. Similar mean metabolic activities were found for the single VNL donor and the 10-donor pool across the studied enzyme markers. On average, the single donor displayed a 1.6-fold higher activity (Figure 5 and Supplemental Table 1) compared to the 10-donor pool. *N*-Acetyl transferase was shown to have 3-fold higher activity in the single donor and CYP2B6 was significantly less active as compared to the 10-donor pool. The higher 1.9-fold AO and 1.6-fold CYP2C9 activities using different small molecules as substrates (diclofenac and O_6-benzyl guanine, respectively) for the metabolic activity determination are in agreement with the higher intrinsic clearance values for tolbutamide (CYP2C9 substrate) and carbazeran (AO substrate). The derived mean metabolic activity index compares enzyme activities across diverse phase I and II hepatic enzymes and can be used to assess donor variability and different in vitro liver systems. This index experiment is independent of the enzyme marker concentration used in the incubation to compare metabolic activity in MPCC hepatocyte or other in vitro liver systems across different test conditions (Supplemental Table 2).

Conclusions and Recommendations

We believe we have identified conditions and protocols that allow for a more facile execution of a MPCC hepatocyte experiment for metabolite identification that also can be designed to generate more data on a single plate. We have determined that the rat media volume can be 400 µL to be consistent across the plate with the other MPCC species. Having one plate with two different sampling volumes added complexity and had the potential for mistakes during the dosing and sampling processes. By showing that the rat media volume no longer needs to be 300 µL, the dosing and sampling of the plate is now far simpler and less prone to sampling error. The metabolite profiles of our test set of compounds were

DMD Fast Forward. Published on July 4, 2020 as DOI: 10.1124/dmd.120.000013
This article has not been copyedited and formatted. The final version may differ from this version.

indistinguishable in rat MPCC between the two volumes tested. In addition to this change, the implementation and use of a cloned dosing plate at 2x drug concentration was also instrumental to the smooth execution of a MPCC hepatocyte metID experiment with less chance of sample handling error.

With the use of the 10-donor human, a new plate design can be envisioned (Figure 6) that combines, human, monkey, dog and rat on the same plate with their respective fibroblast controls. This design allows for the dog MPCC to be directly adjacent to the respective controls.

Similar metabolic activity was found for the single VNL donor and the 10-donor pool across studied enzyme markers. The observed difference in enzyme activities are likely due to donor variability. With the investigation of only one single and 10-donor pooled human MPCC hepatocyte, our conclusion regarding the equivalence of the test systems are however limited and further investigations of new donors will help to substantiate our findings.

The use of the 10-donor human MPCC pool protects against any seeding, plating and activity discrepancies that may occur with a single donor and also protects against any inter-individual variability. Additional research to identify higher average activity donors to maximize overall enzyme activities would aid in the production of more robust metabolite profiles for comparison to in vivo preclinical and clinical samples to support IVIVC translation.

Acknowledgements

The authors would like to thank Stacy Krzyzewski, Onyi Irrechukwu, Jeannemarie Gaffney and Jack McGeehan from Ascendance Biotechnologies/BioIVT for supplying the MPCC plates and for helpful discussions.

Authorship Contributions

Participated in research design: Ballard, Kratochwil, Cox, Moen. Klammers

Conducted experiments: Cox, Moen, Klammers, Ekiciler, Goetschi, Walter

Performed data analysis: Ballard, Kratochwil, Klammers

DMD Fast Forward. Published on July 4, 2020 as DOI: 10.1124/dmd.120.000013
This article has not been copyedited and formatted. The final version may differ from this version.

Wrote or contributed to the writing of the manuscript: Ballard, Kratochwil, Cox, Moen, Klammers, Ekiciler, Goetschi, Walter

DMD Fast Forward. Published on July 4, 2020 as DOI: 10.1124/dmd.120.000013
This article has not been copyedited and formatted. The final version may differ from this version.

References

Back DJ and Orme ML (1989) Genetic factors influencing the metabolism of tolbutamide. *Pharmacol Ther* **44:**147-155.

Ballard TE, Orozco CC, and Obach RS (2014) Generation of major human excretory and circulating drug metabolites using a hepatocyte relay method. *Drug Metab Dispos* **42:**899-902.

Ballard TE, Wang S, Cox LM, Moen MA, Krzyzewski S, Ukairo O, and Obach RS (2016) Application of a Micropatterned Cocultured Hepatocyte System To Predict Preclinical and Human-Specific Drug Metabolism. *Drug Metab Dispos* **44:**172-179.

Bonn B, Svanberg P, Janefeldt A, Hultman I, and Grime K (2016) Determination of Human Hepatocyte Intrinsic Clearance for Slowly Metabolized Compounds: Comparison of a Primary Hepatocyte/Stromal Cell Co-culture with Plated Primary Hepatocytes and HepaRG. *Drug Metab Dispos* **44:**527-533.

Burton RD, Hieronymus T, Chamem T, Heim D, Anderson S, Zhu X, and Hutzler JM (2018) Assessment of the Biotransformation of Low-Turnover Drugs in the HmicroREL Human Hepatocyte Coculture Model. *Drug Metab Dispos* **46:**1617-1625.

Chan TS, Yu H, Moore A, Khetani SR, and Tweedie D (2013) Meeting the challenge of predicting hepatic clearance of compounds slowly metabolized by cytochrome P450 using a novel hepatocyte model, HepatoPac. *Drug Metab Dispos* **41:**2024-2032.

Dalvie D, Obach RS, Kang P, Prakash C, Loi CM, Hurst S, Nedderman A, Goulet L, Smith E, Bu HZ, and Smith DA (2009) Assessment of three human in vitro systems in the generation of major human excretory and circulating metabolites. *Chem Res Toxicol* **22:**357-368.

Dash A, Inman W, Hoffmaster K, Sevidal S, Kelly J, Obach RS, Griffith LG, and Tannenbaum SR (2009) Liver tissue engineering in the evaluation of drug safety. *Expert Opin Drug Metab Toxicol* **5:**1159-1174.

Di L and Obach RS (2015) Addressing the challenges of low clearance in drug research. *AAPS J* **17:**352-357.

Gee SJ, Green CE, and Tyson CA (1984) Comparative metabolism of tolbutamide by isolated hepatocytes from rat, rabbit, dog, and squirrel monkey. *Drug Metab Dispos* **12:**174-178.

Heyward S, McCauley P, Moeller T, (2016) Utility of pooled cryoplateable LIVERPOOL™ in the in vitro determination of cytochrome P450 metabolism and induction. 20th North American ISSX Meeting: P184. *Drug Metab Rev* **48:**28-28.

Hultman I, Vedin C, Abrahamsson A, Winiwarter S, and Darnell M (2016) Use of HμREL Human Coculture System for Prediction of Intrinsic Clearance and Metabolite Formation for Slowly Metabolized Compounds. *Mol Pharm* **13:**2796-2807.

Hutzler JM, Ring BJ, and Anderson SR (2015) Low-Turnover Drug Molecules: A Current Challenge for Drug Metabolism Scientists. *Drug Metab Dispos* **43:**1917-1928.

Jones HMC, Y.; Gibson, C.; Heimbach, T.; Parrott, N.; Peters, S. A.; Snoeys, J.; Upreti, V. V.; Zheng, M.; Hall, S. D. (2015) Physiologically based pharmacokinetic modeling in drug discovery and development: A pharmaceutical industry perspective. *Clin Pharmacol Ther* **97:**247-262.

Kaye B, Offerman JL, Reid JL, Elliott HL, and Hillis WS (1984) A species difference in the presystemic metabolism of carbazeran in dog and man. *Xenobiotica* **14:**935-945.

Kerns EHD, L. (2008) *Drug-like properties: concepts, structure design, and methods: from ADME to toxicity optimization*. Academic Press, Burlington, Massachusetts.

Khetani SR and Bhatia SN (2008) Microscale culture of human liver cells for drug development. *Nat Biotechnol* **26:**120-126.

Kratochwil NA, Meille C, Fowler S, Klammers F, Ekiciler A, Molitor B, Simon S, Walter I, McGinnis C, Walther J, Leonard B, Triyatni M, Javanbakht H, Funk C, Schuler F, Lave T, and Parrott NJ (2017)

Metabolic Profiling of Human Long-Term Liver Models and Hepatic Clearance Predictions from In Vitro Data Using Nonlinear Mixed-Effects Modeling. *AAPS J* **19:**534-550.

Lombardo F, Waters NJ, Argikar UA, Dennehy MK, Zhan J, Gunduz M, Harriman SP, Berellini G, Liric Rajlic I, and Obach RS (2013) Comprehensive assessment of human pharmacokinetic prediction based on in vivo animal pharmacokinetic data, part 2: clearance. *J Clin Pharmacol* **53:**178-191.

Pelkonen O and Raunio H (2005) In vitro screening of drug metabolism during drug development: can we trust the predictions? *Expert Opin Drug Metab Toxicol* **1:**49-59.

Plant N (2004) Strategies for using in vitro screens in drug metabolism. *Drug Discov Today* **9:**328-336.

Wang WW, Khetani SR, Krzyzewski S, Duignan DB, and Obach RS (2010) Assessment of a micropatterned hepatocyte coculture system to generate major human excretory and circulating drug metabolites. *Drug Metab Dispos* **38**:1900-1905.

DMD Fast Forward. Published on July 4, 2020 as DOI: 10.1124/dmd.120.000013
This article has not been copyedited and formatted. The final version may differ from this version.

Footnotes

Footnote 1: No concentration dependency of Cl_{int} was observed for carbazeran in MPCC hepaptocyes (single or 10-donor) in contrast to suspension hepatocytes (*details are given in the supplementary material*).

DMD Fast Forward. Published on July 4, 2020 as DOI: 10.1124/dmd.120.000013
This article has not been copyedited and formatted. The final version may differ from this version.

Legends for Figures

Figure 1. Set of test compounds to be used in this analysis.

Figure 2. Representative UV-UHPLC chromatograms of carbazeran metabolism in rat MPCC hepatocytes. BG: Background.

Figure 3. Metabolic scheme of carbazeran in rat and human MPCC hepatocytes. Position of catechol demethylation and subsequent conjugation not known. 4-Position oxo-carbazeran and des-ethyl metabolites (*m/z* 333, *m/z* 349 and *m/z* 377) and 3-*N*-conjugate metabolite structures (*m/z* 523b and *m/z* 537) inferred from literature (Kaye et al., 1984).

Figure 4. Representative UV-UHPLC chromatograms of carbazeran metabolism in single and 10-donor MPCC hepatocytes. BG: Background.

Figure 5. Metabolic profiling of single vs. 10-donor MPCC hepatocytes with selective enzyme substrates. Line represents the mean of the derived metabolic activity index values. Similar mean metabolic activities were found for the single VNL donor and the 10-donor pool with average values of 58 and 37, respectively.

Figure 6. Proposed multispecies MPCC hepatocyte plate including 10-donor human and fibroblast controls for all plated species. Time point A = Day 0, 0h media removal; B = Day 2 media and cells; C = Day 7 media and cells. (MsF: mouse fibroblasts, mH: mouse hepatocytes, HuF: human fibroblasts).

DMD Fast Forward. Published on July 4, 2020 as DOI: 10.1124/dmd.120.000013
This article has not been copyedited and formatted. The final version may differ from this version.

Tables

Table 1. Intrinsic clearance determinations for the test set of compounds. RSE%: Relative Standard Error.

Compounds	Enzyme markers	Conc. (μM)	Cl_{int} (μL $min^{-1}mg^{-1}$protein)	
			VNL Donor (RSE%)	Multiple Donor Pool (RSE%)
Carbazeran	AO	0.3-3	79.9 (4)	57.5 (4)
Sunitinib	CYP3A4	1	10.0 (1)	9.9 (2)
Tolbutamide	CYP2C9	1	4.6 (4)	1.7 (10)
Trifluoperazine	UGT1A4	0.3	25.8 (4)	24.8 (2)
Quinidine	CYP3A4	1	13.6 (4)	13.5 (4)

DMD Fast Forward. Published on July 4, 2020 as DOI: 10.1124/dmd.120.000013
This article has not been copyedited and formatted. The final version may differ from this version.

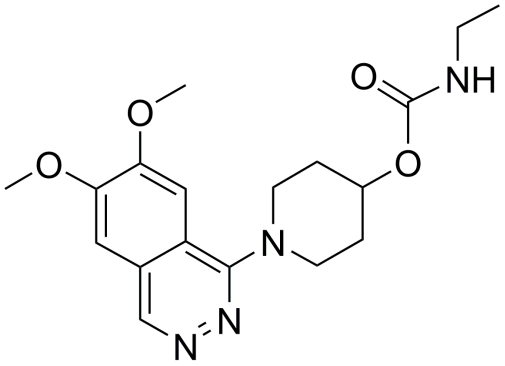

carbazeran

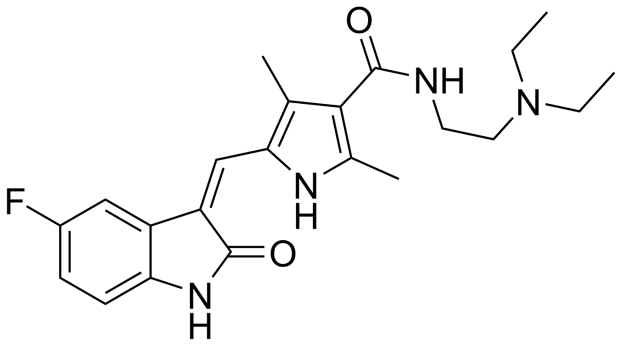

sunitinib

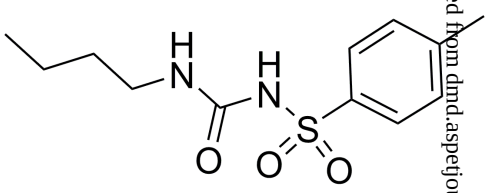

tolbutamide

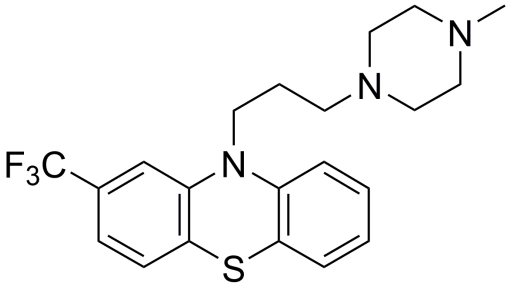

trifluoperazine

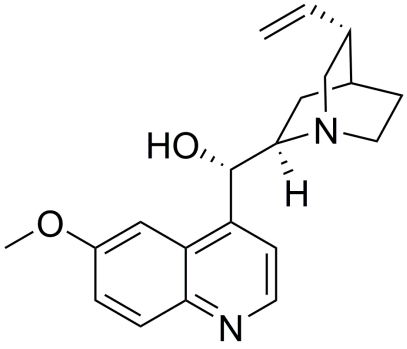

quinidine

DMD Fast Forward. Published on July 4, 2020 as DOI: 10.1124/dmd.120.000013
This article has not been copyedited and formatted. The final version may differ from this version.

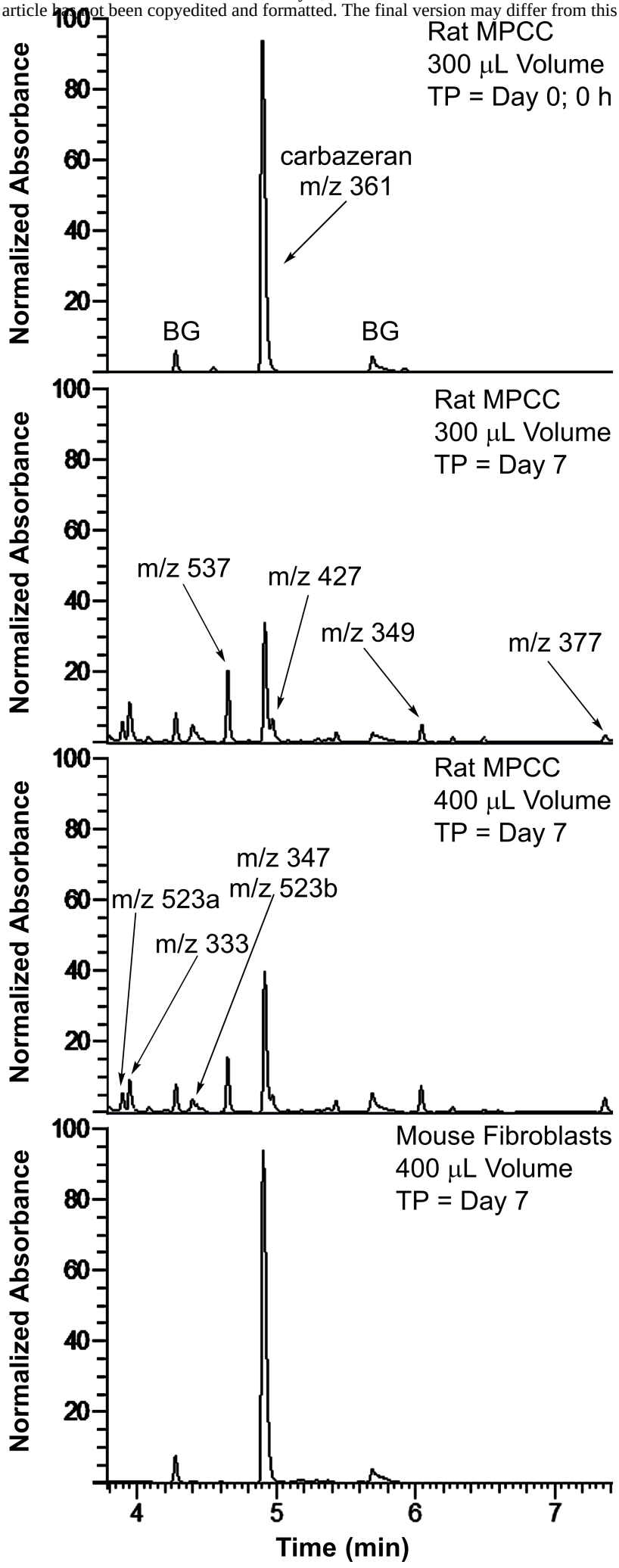

DMD Fast Forward. Published on July 4, 2020 as DOI: 10.1124/dmd.120.000013
This article has not been copyedited and formatted. The final version may differ from this version.

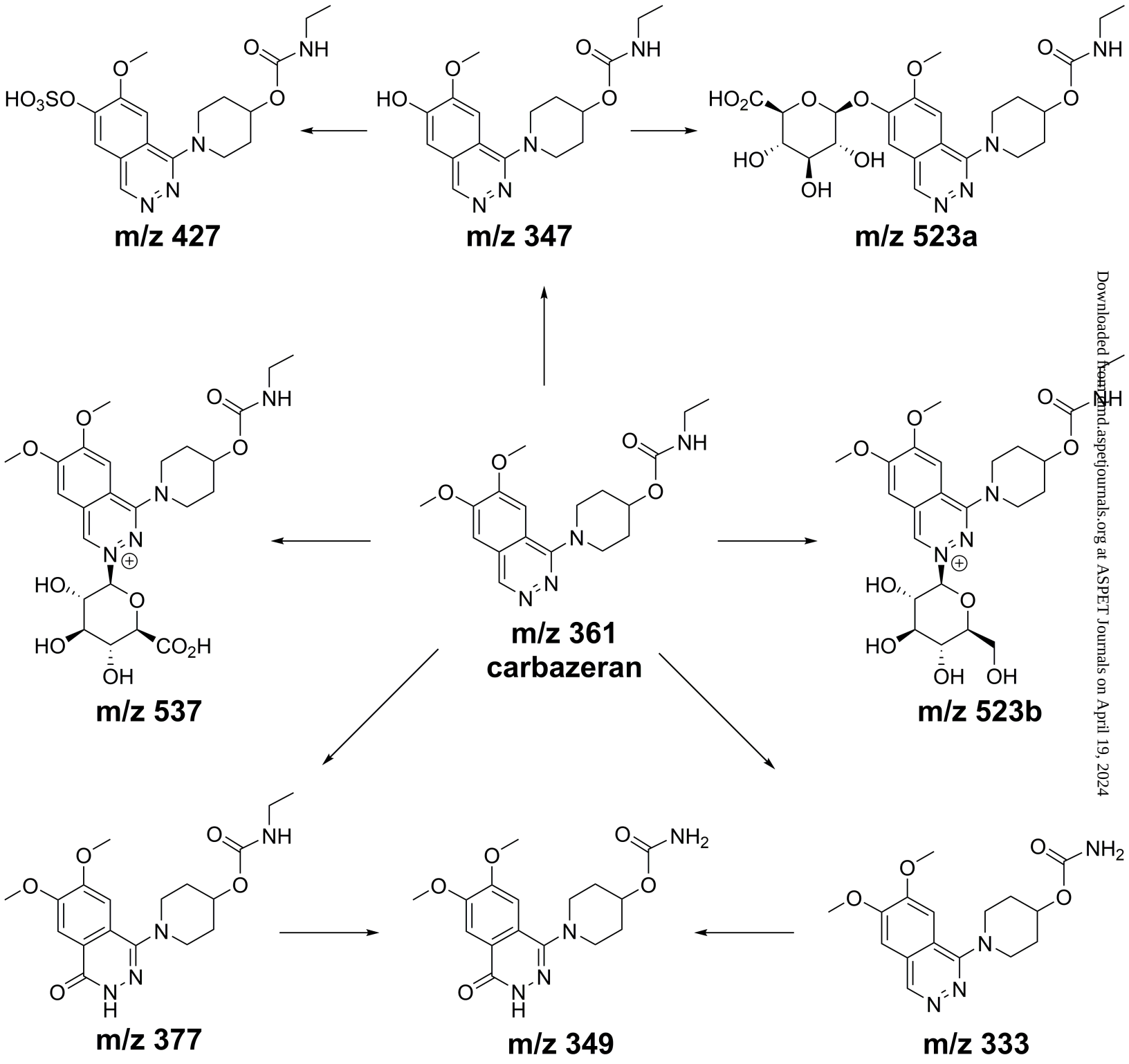

DMD Fast Forward. Published on July 4, 2020 as DOI: 10.1124/dmd.120.000013
This article has not been copyedited and formatted. The final version may differ from this version.

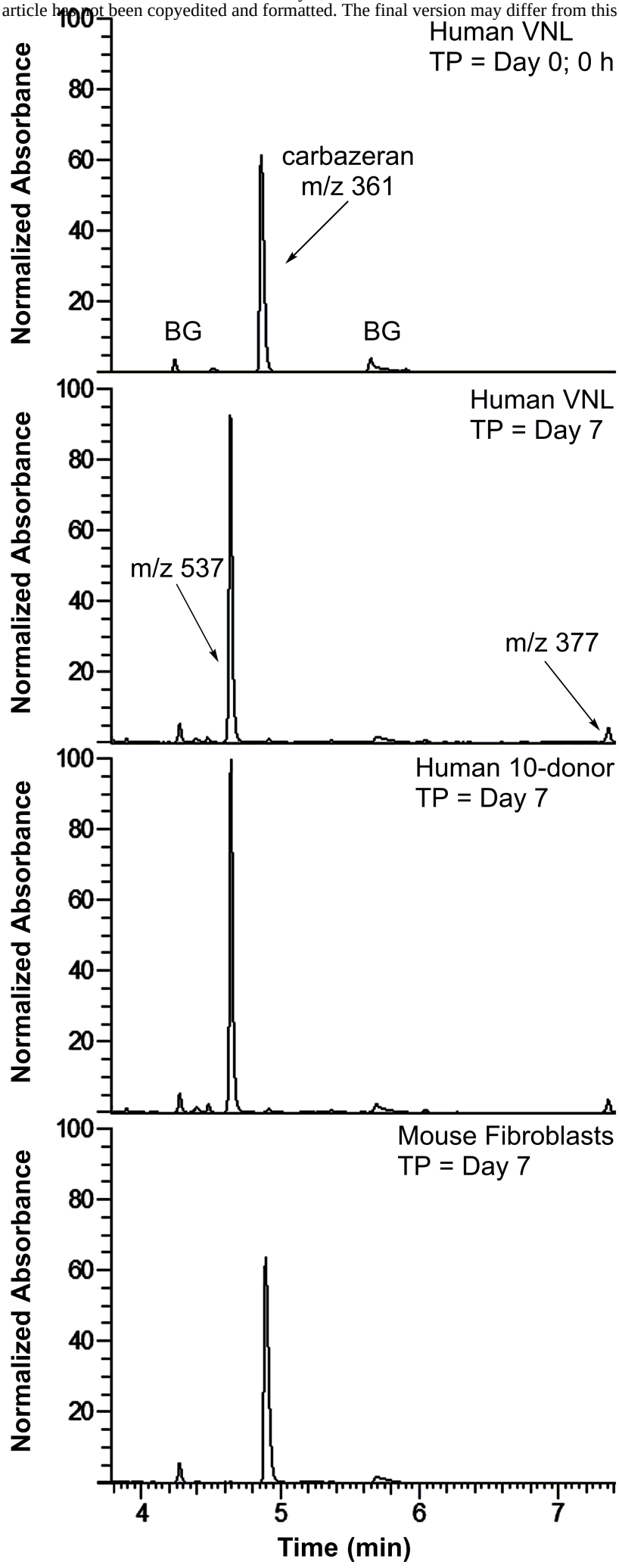

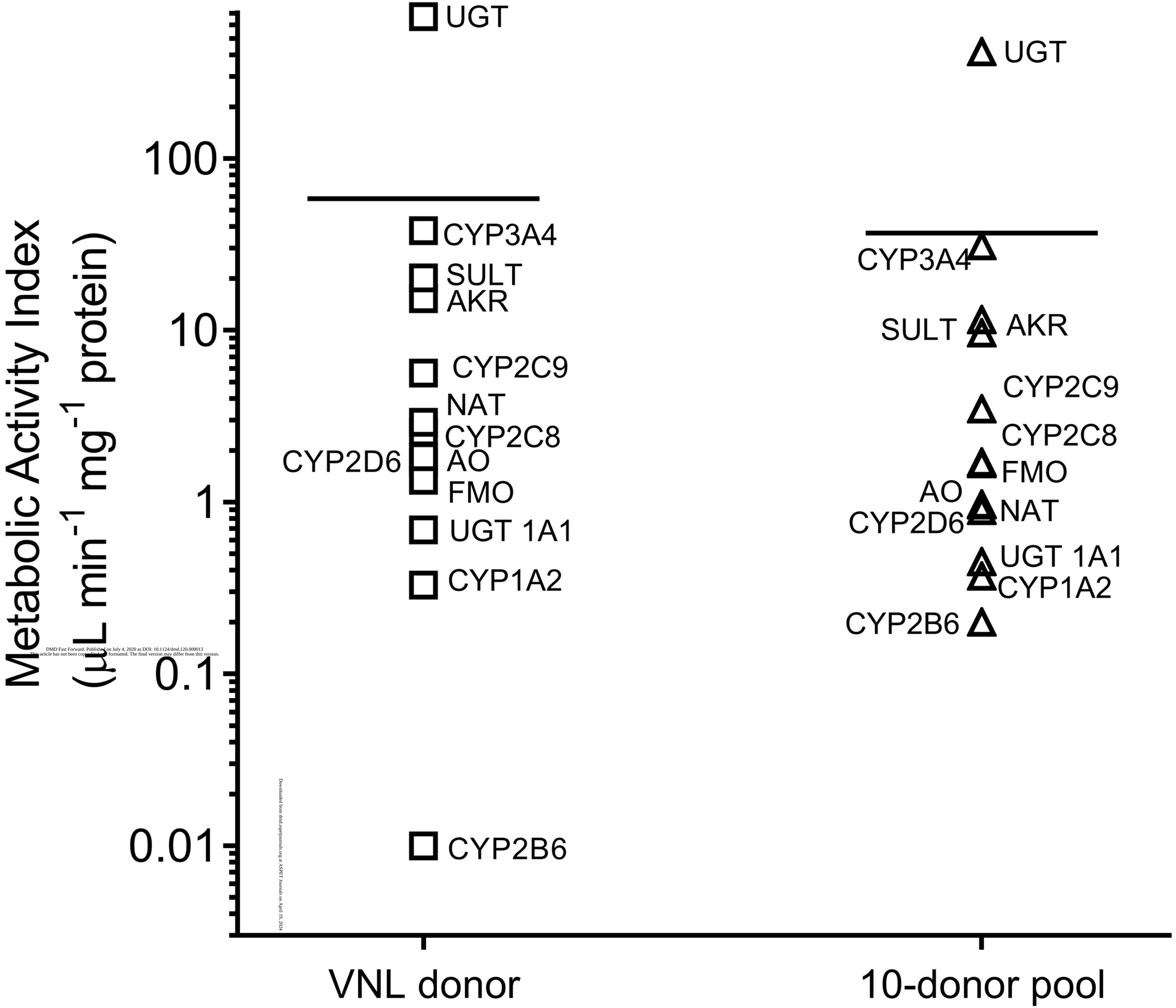

DMD Fast Forward. Published on July 4, 2020 as DOI: 10.1124/dmd.120.000013
This article has not been copyedited and formatted. The final version may differ from this version.

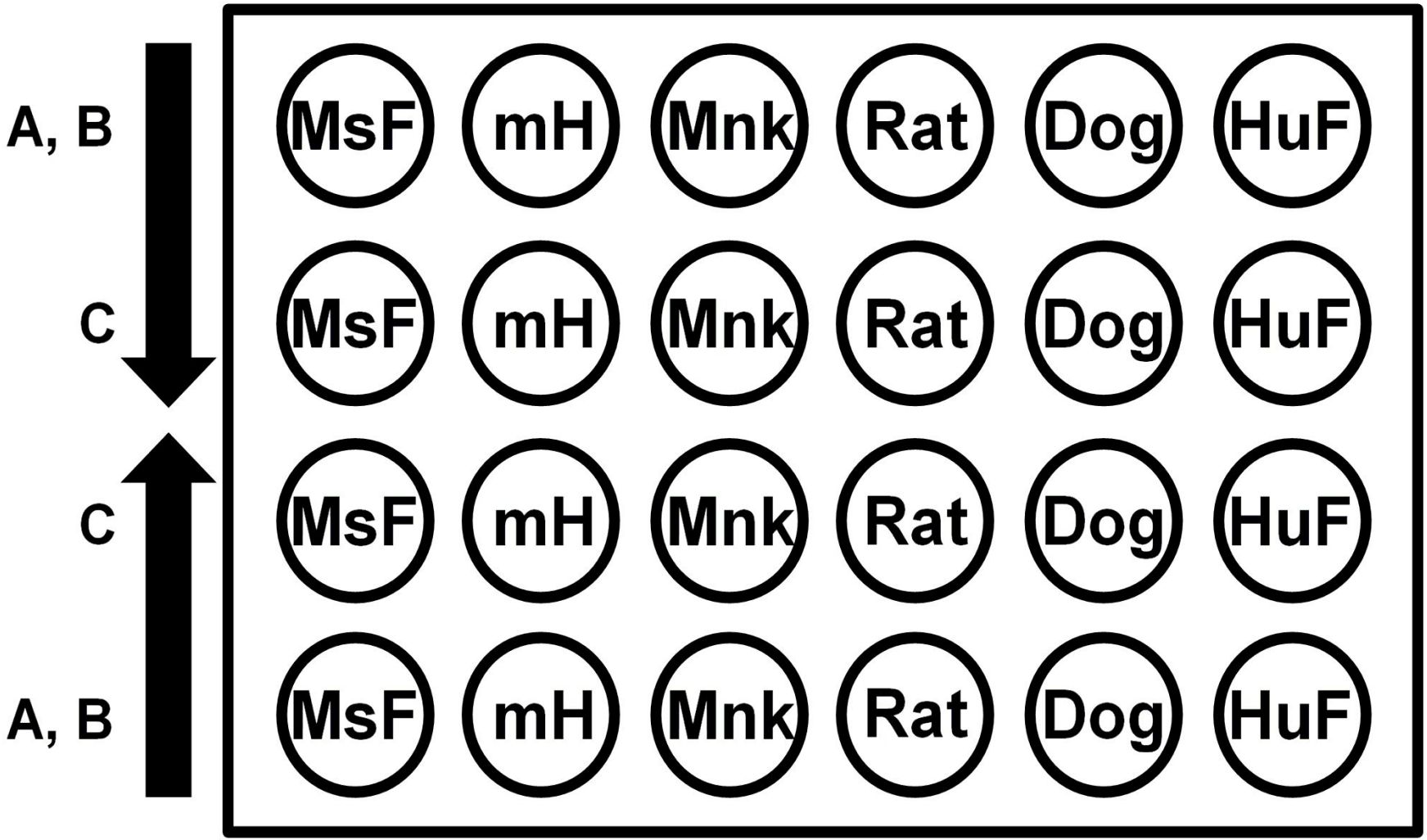
Time Points
A, B
C
C
A, B
MsF
mH
Mnk
Rat
Dog
HuF

Supplementary Material

Simplifying the Execution of HepatoPac MetID Experiments: Metabolite Profile and Intrinsic Clearance Comparisons

T. Eric Ballard, N. Kratochwil, Loretta M. Cox, Mark A. Moen, F. Klammers, A. Ekiciler, A. Goetschi and I. Walter

Global Drug Metabolism and Pharmacokinetics, Takeda Pharmaceuticals Co., Cambridge, MA 02139, USA; TEB (Current)

Pharmacokinetics, Dynamics and Metabolism, Pfizer, Inc., Groton, CT 06340, USA; TEB, LMC, MAM

Drug Disposition and Safety, Roche Pharmaceutical Research and Early Development, Roche Innovation Center, 4070 Basel CH, Switzerland; NK, FK, AE, AG, IW

Supplemental Figure 1. Representative UV-UHPLC chromatograms of sunitinib metabolism in rat MPCC hepatocytes.

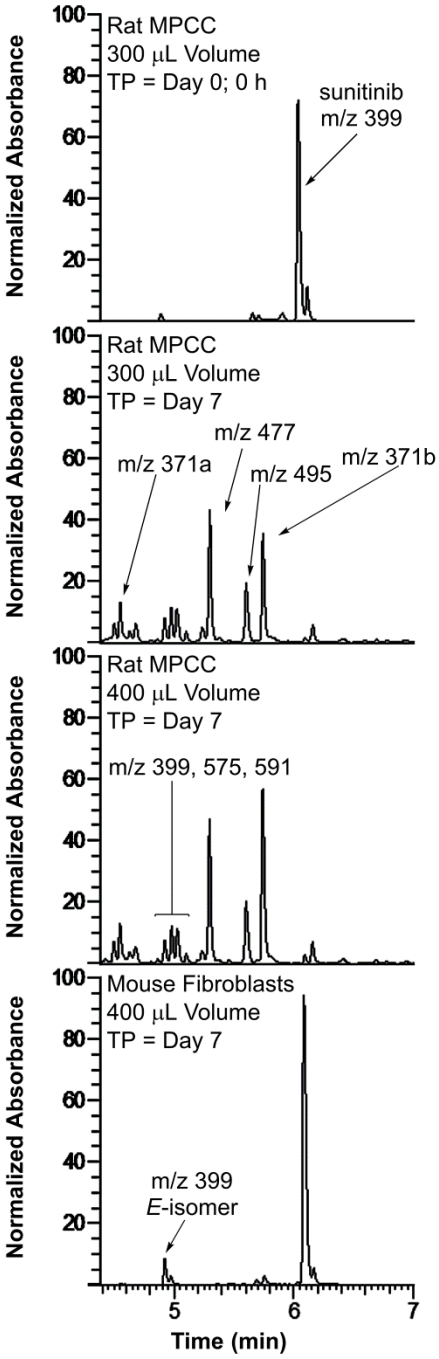

Supplemental Figure 2. Representative UV-UHPLC chromatograms of tolbutamide metabolism in rat MPCC hepatocytes.

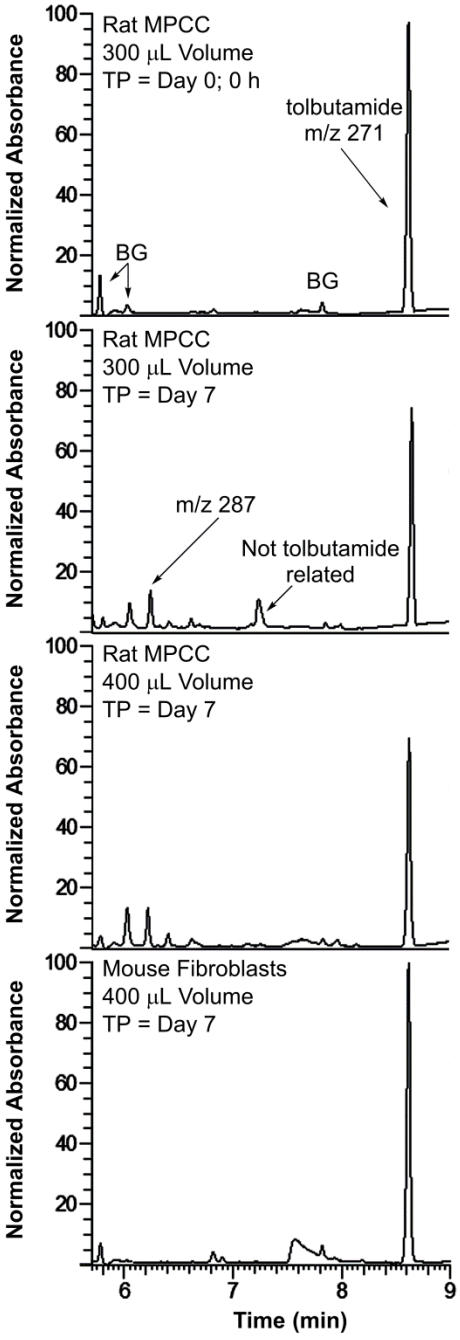

Supplemental Figure 3. Representative UV-UHPLC chromatograms of trifluoperazine metabolism in rat MPCC hepatocytes.

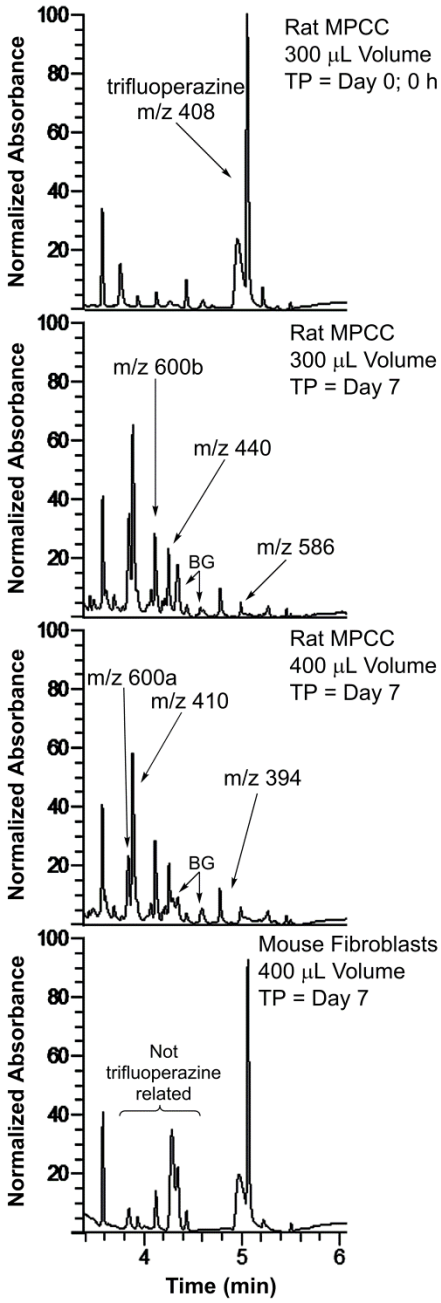

Supplemental Figure 4. Representative UV-UHPLC chromatograms of quinidine metabolism in rat MPCC hepatocytes.

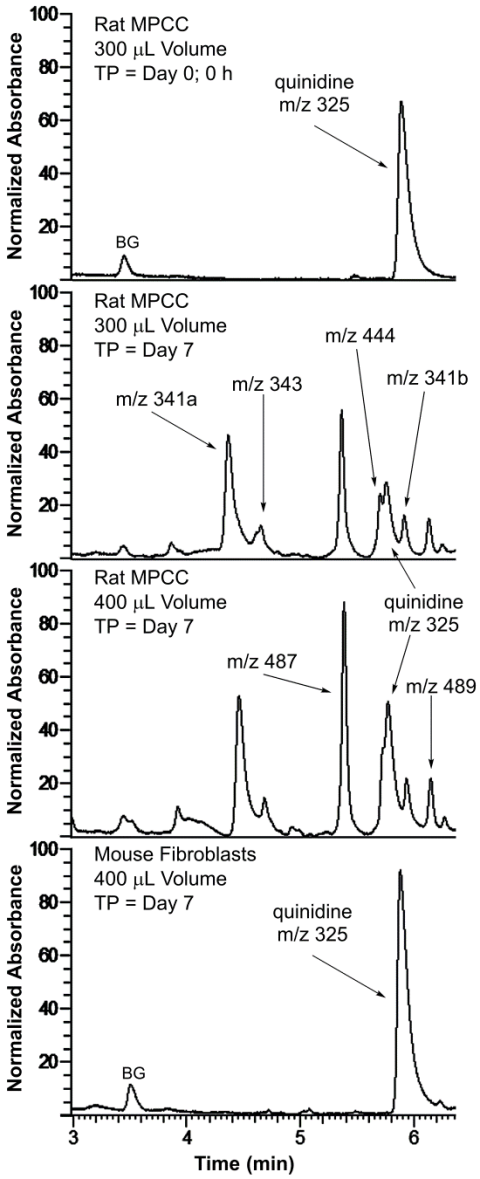

Supplemental Figure 5. Metabolic scheme of sunitinib in rat and human MPCC hepatocytes.

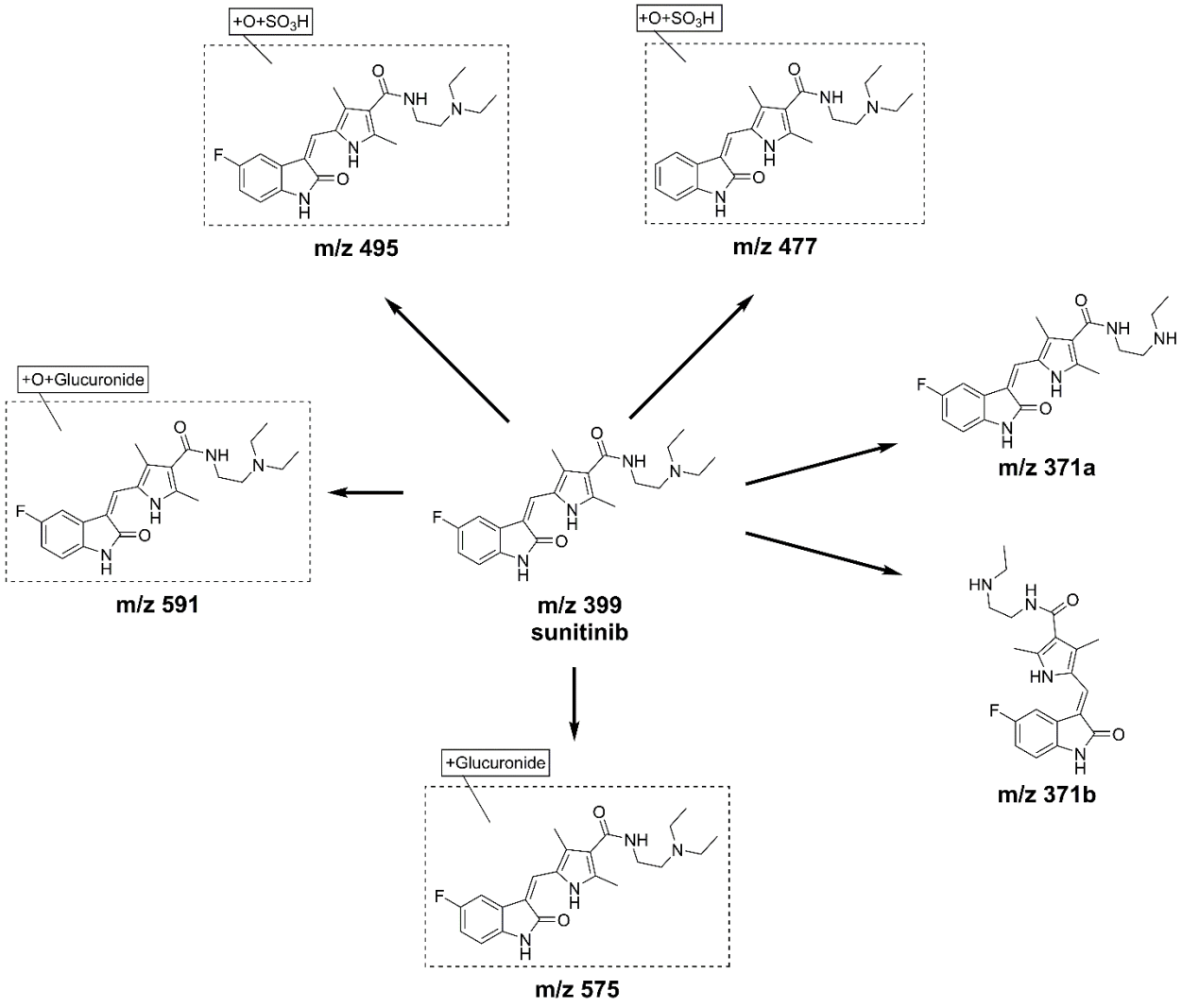

Supplemental Figure 6. Metabolic scheme of tolbutamide in rat and human MPCC hepatocytes.

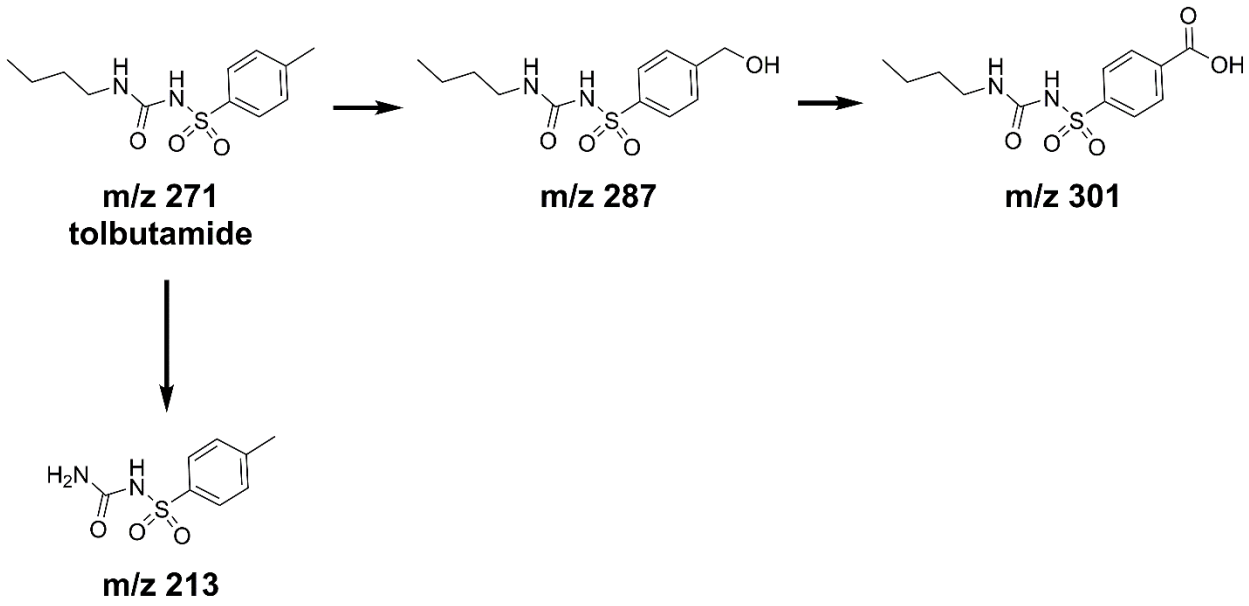

Supplemental Figure 7. Metabolic scheme of trifluoperazine in rat and human MPCC hepatocytes.

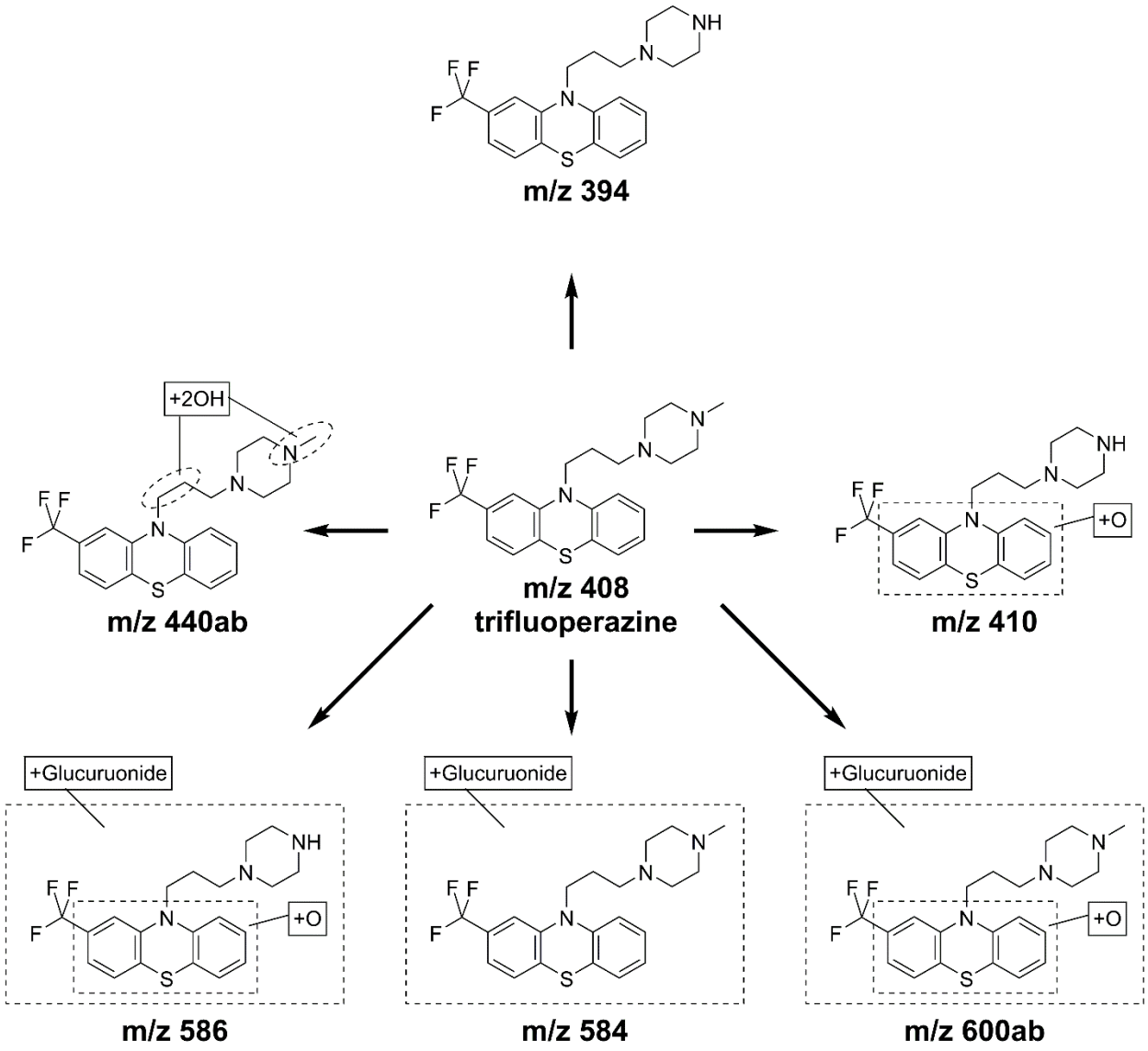

Supplemental Figure 8. Metabolic scheme of quinidine in rat and human MPCC hepatocytes.

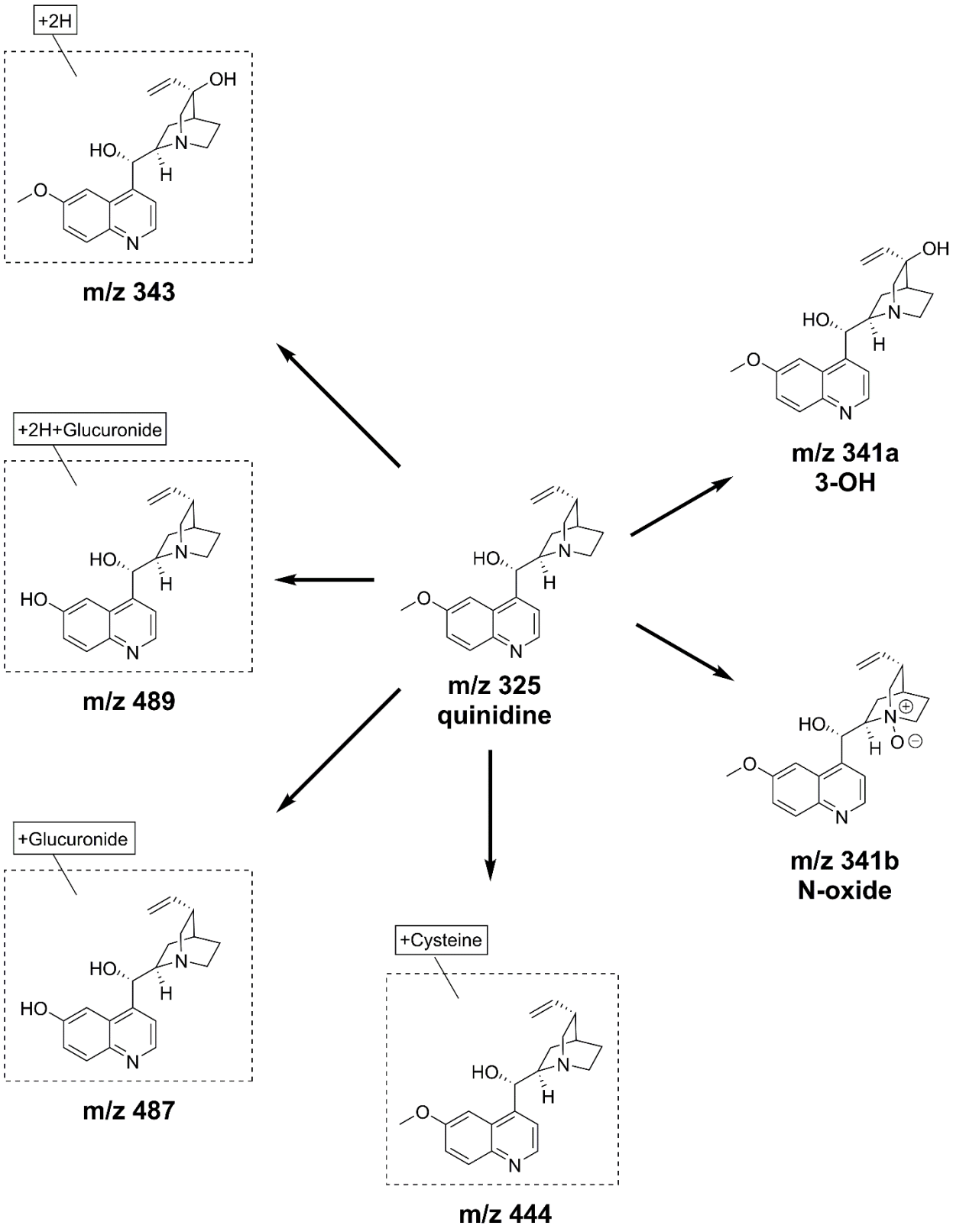

Supplemental Figure 9. Tolbutamide metabolism in rat MPCC hepatocytes; representative extracted ion chromatograms (XICs) for urea dealkylation metabolite (m/z 213.0339; negative ion mode).

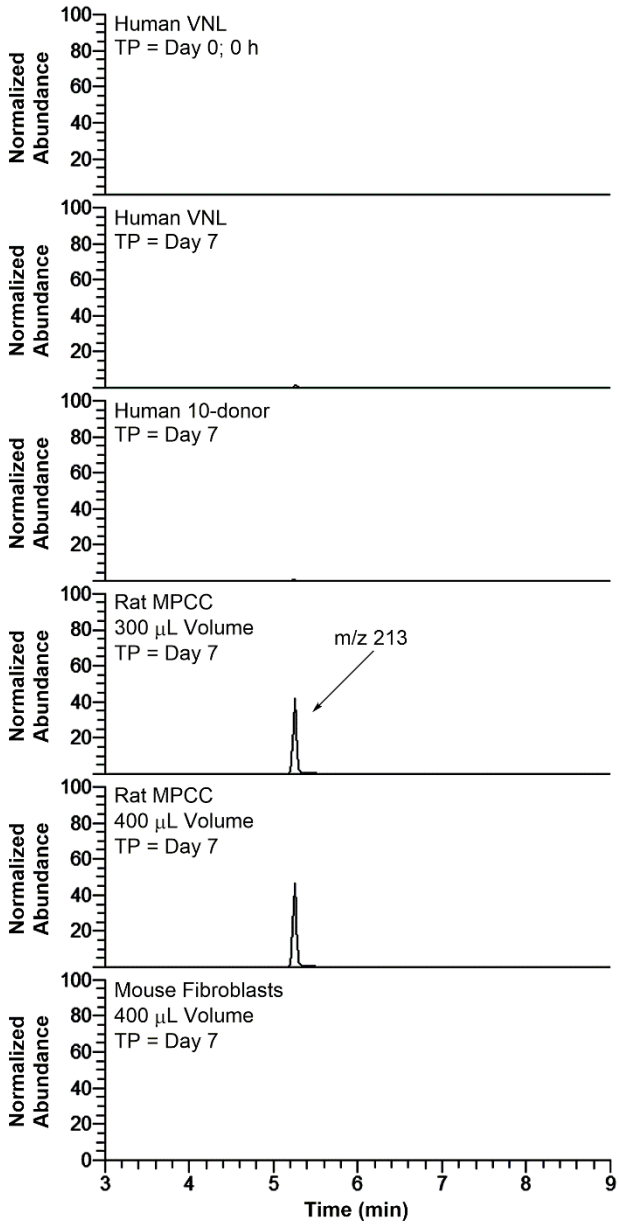

Supplemental Figure 10. Time vs concentration plots used to generate intrinsic clearance in HepatoPac® plates. Lines present predictions applying pharmacokinetic modeling using a nonlinear mixed-effects approach.

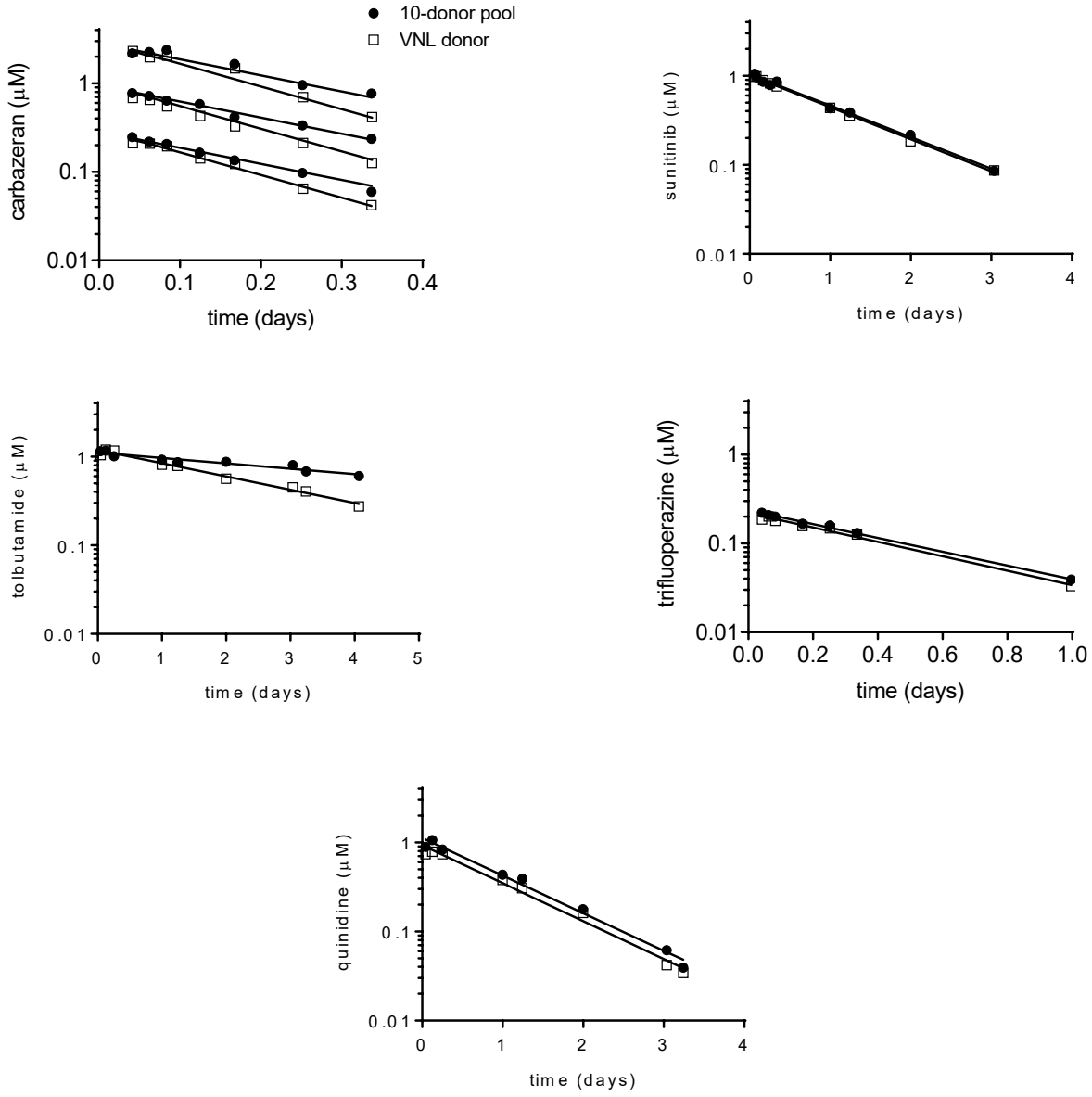

Supplemental Figure 10a. Time vs concentration plots in mouse embryonic 3T3 fibroblast only control plates for correction of the derived intrinsic clearance values in HepatoPac® plates (shown in Supplemental Figure 10)

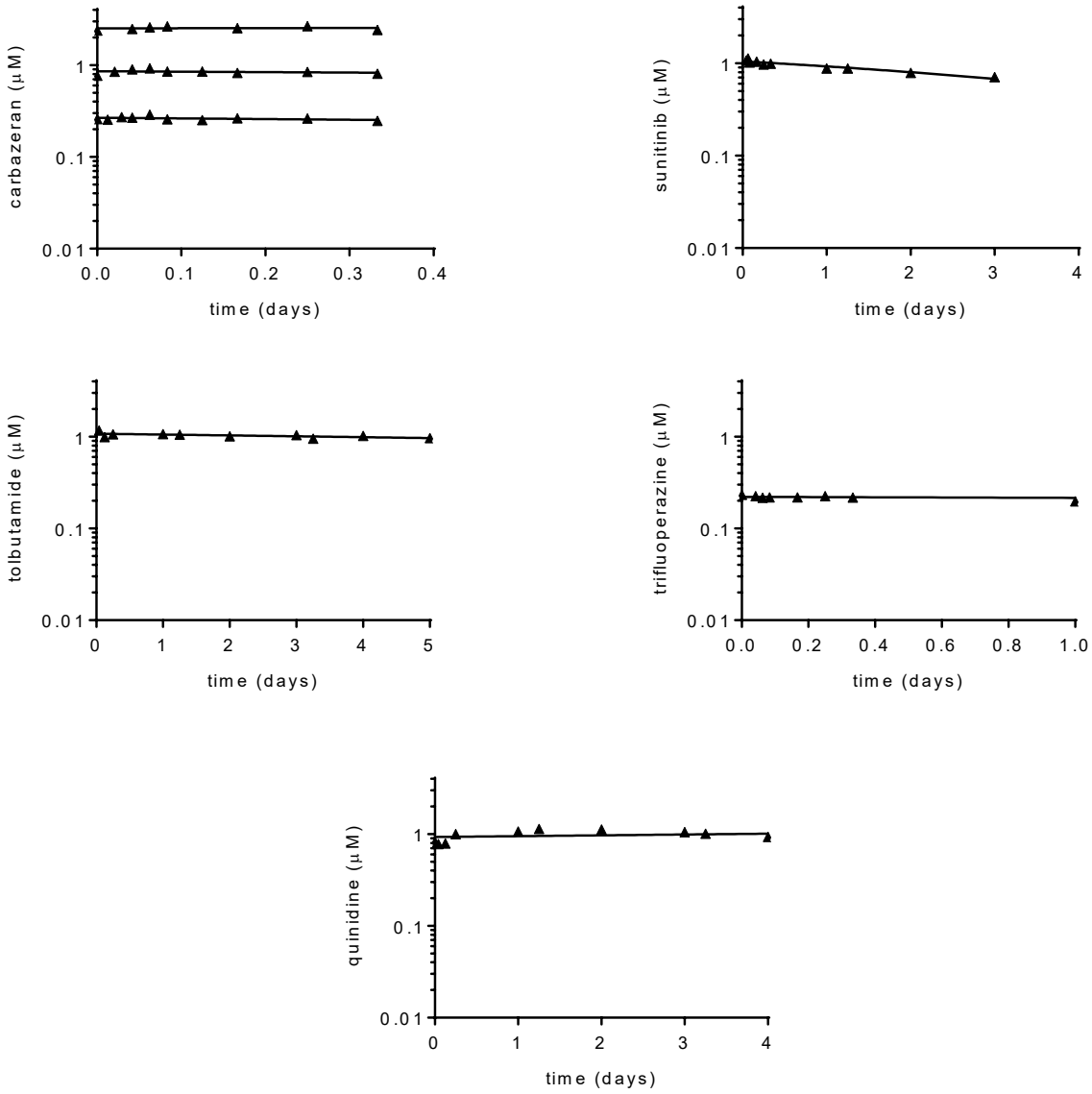

Supplemental Figure 11. Representative UV-UHPLC chromatograms of tolbutamide metabolism in single and 10-donor MPCC hepatocytes.

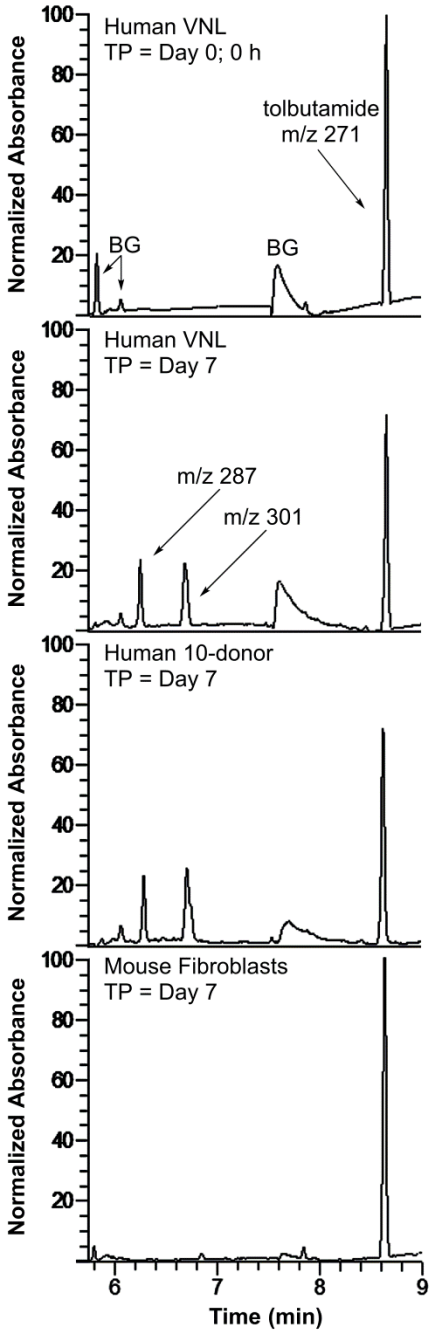

Supplemental Figure 12. Representative UV-UHPLC chromatograms of sunitinib metabolism in single and 10-donor MPCC hepatocytes.

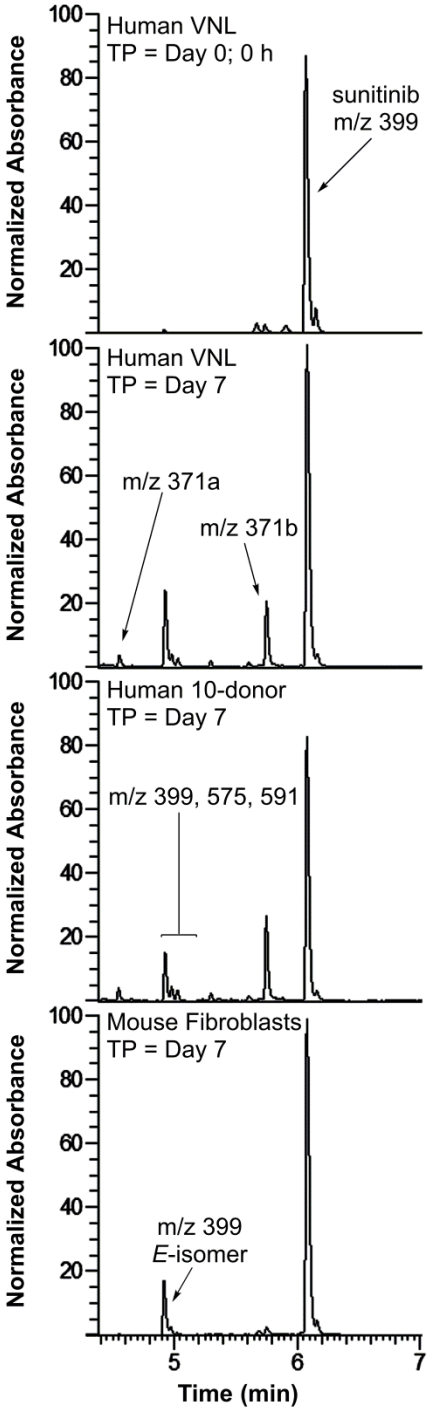

Supplemental Figure 13. Representative UV-UHPLC chromatograms of trifluoperazine metabolism in single and 10-donor MPCC hepatocytes.

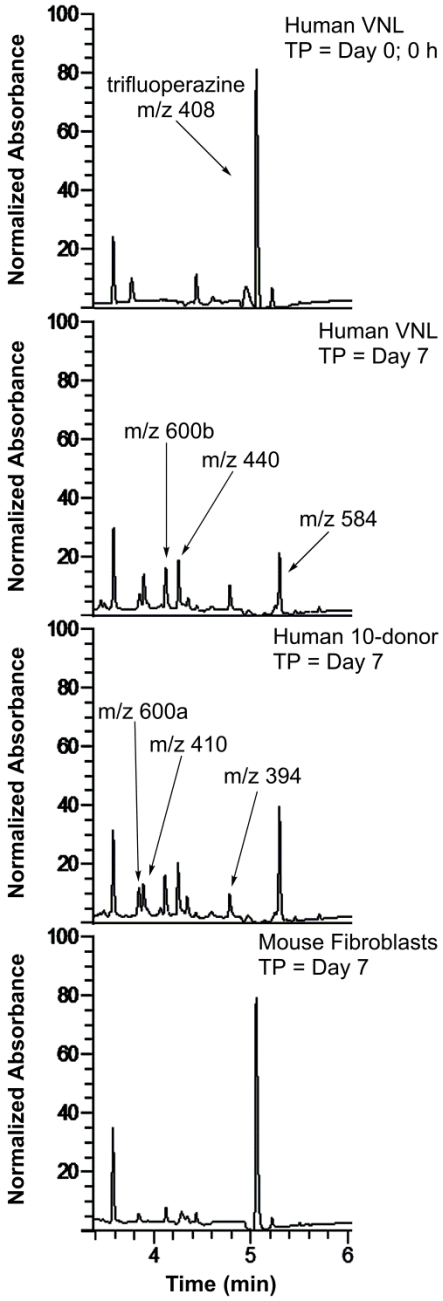

Supplemental Figure 14. Representative UV-UHPLC chromatograms of quinidine metabolism in single and 10-donor MPCC hepatocytes.

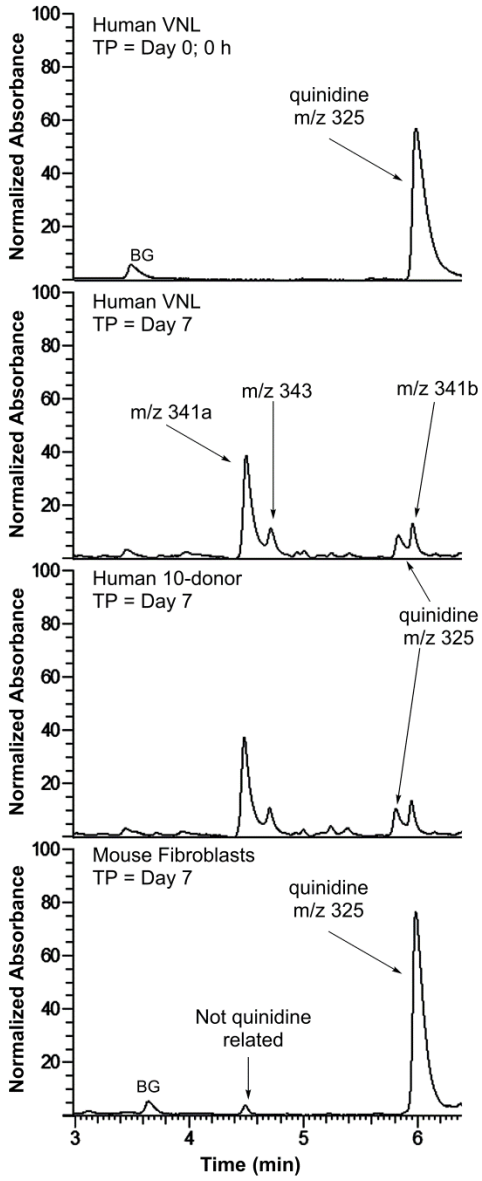

Supplemental Table 1. Metabolic profiling of single vs. 10-donor MPCC hepatocytes with selective enzyme substrates tabular data.

Major Metabolic Enzyme	Incubated compounds	Conc. (µM)	Analyzed enzyme markers	Metabolite formation rate Single Donor VNL (pmol $min^{-1}mg^{-1}$protein)	Metabolite formation rate Multiple Donors (pmol $min^{-1}mg^{-1}$protein)
CYP3A4	midazolam	5	1'-hydroxymidazolam	190.4	154.8
CYP2D6	dextromethorphan	5	dextrophan	8.6	4.5
CYP2C9	diclofenac	10	4-hydroxydiclofenac	56.3	34.9
CYP2B6	bupropion	20	hydroxybuproprion	0.3	4.0
CYP1A2	tacrine	10	hydroxytacrine	3.3	3.7
CYP2C8	amodiaquine	20	N-desethylamodiaquine	51.5	33.4
FMO	benzydamine	1	benzydamine N-oxide	1.3	1.7
AKR	daunorubicin	10	daunorubicinol	152.8	96.3
AO	O_6-benzylguanine	10	8-oxo-O_6-benzylguanine	18.4	9.6
NAT	sulfamethazine	20	N-acetyl-sulfamethazine	58.2	19.4
UGT 1A1	SN-38	50	SN-38 glucuronide	34.6	22.4
SULT	7-	10	7-hydroxycoumarin sulfate	202.4	114.8
UGT	7-hydroxycoumarin	10	7-hydroxycoumarin glucuronide	6686.9	4169.0

Supplemental Table 2. Metabolic Activity Index (activity is independent of substrate concentration).

Responsible metabolic enzyme	Incubated compounds	Analyzed enzyme markers	Metabolic Activity Index HepatoPac (VNL) (µL $min^{-1}mg^{-1}$protein)	Metabolic Activity Index HepatoPac Multiple Donors (µL $min^{-1}mg^{-1}$protein)
CYP3A4	midazolam	1'-hydroxymidazolam	38.1	30.9
CYP2D6	dextromethorphan	dextrophan	1.7	0.9
CYP2C9	diclofenac	4-hydroxydiclofenac	5.6	3.5
CYP2B6	bupropion	hydroxybuproprion	0.01	0.2
CYP1A2	tacrine	hydroxytacrine	0.3	0.4
CYP2C8	amodiaquine	N-desethylamodiaquine	2.6	1.7
FMO	benzydamine	benzydamine N-oxide	1.3	1.7
AKR	daunorubicin	daunorubicinol	15.3	9.6
AO	O_6-benzylguanine	8-oxo-O_6-benzylguanine	1.8	0.9
NAT	sulfamethazine	N-acetyl-sulfamethazine	2.9	0.9
UGT 1A1	SN-38	SN-38 glucuronide	0.7	0.5
SULT	7-hydroxycoumarin	7-hydroxycoumarin sulfate	20.3	11.5
UGT	7-hydroxycoumarin	7-hydroxycoumarin glucuronide	668.7	416.9

Supplemental Table 3: MS setting for Clint.

Detection was achieved in positive ion MRM mode with the following parameter settings:

Analyte Name	Q1 Mass (m/z)	Q3 Mass (m/z)	Collision Energy (V)	Retention Time (min)
RO0053842-001-001 (Trifluoperazine)	408.20	141.10	31	0.79
RO0029697-000-001 (Tolbutamide)	271.05	91.10	43	0.82
RO4632993-001-001 (Sunitinib)	399.17	283.10	35	0.73/0.76
Carbazeran	361.14	272.10	27	0.72
RO00120633-000-001 (Quinidine)	325.14	307.10	31	0.66
RO0056789-000 (Oxazepam)	287.1	241.1	31	0.81
hydroxyl buproprion	256.00	238.10	17	0.71
1'-hydroxy midazolam	342.00	323.95	35	0.74
dextrorphan	258.10	157.10	53	0.68
hydroxytacrine	215.10	197.10	25	0.69
7-hydroxy coumarin glucuronide	337.00	161.00	-30	0.86
7-hydroxy coumarin sulfate	240.90	161.00	-24	0.85
4-hydroxy diclofenac	312.00	230.10	45	0.81
benzydamine N-oxide	326.10	102.10	21	0.75
daunorubicinol	530.15	383.00	19	0.76
8-oxo-O6-benzylguanine	258.04	91.00	37	0.76
SN-38 glucuronide	569.12	393.10	39	0.71
N-acetyl sulfamethazine	321.05	186.10	29	0.72

Supplemental Table 4: Intrinsic Clearance Values for Carbazeran in Hepatocyte Suspension Cultures (Multiple Donors)

Compound	Enzyme markers	Dose (μM)	Clint (μL/min/mg Protein)	
Carbazeran	AO	0.3 – 10	* **	3.3 – 65 11 – 96

Human Hepatocytes from Bioreclamation *Batch: RBR , **Batch: JJR

Plate Maps. Plates 1 - 4 contain carbazeran, sunitinib, tolbutamide and trifluoperazine on each plate. Plates 1 and 2 compare human VNL and the 10-donor pool with fibroblast controls. Plates 3 and 4 assess rat Hepatopac and respective controls. Plate 5 is quinidine alone as a combination plate with assessment of human and rat hepatopac and controls.

Plate 1

Human Donor VNL HepatoPac			Stromal Only Controls for Human HepatoPac - 3T3 J2 Mouse Fibroblasts		
1 DMSO t0/t2	2 Sunitinib t0/t2	3 Carbazeran t0/t2	4 Sunitinib t0/t2	5 Carbazeran t0/t2	6 DMSO t0/t2
1 DMSO t7	2 Sunitinib t7	3 Carbazeran t7	4 Sunitinib t7	5 Carbazeran t7	6 DMSO t7
7 DMSO t7	8 tolbutamide t7	9 Trifluoperazine t7	10 tolbutamide t7	11 Trifluoperazine t7	12 DMSO t7
7 DMSO t0/t2	8 tolbutamide t0/t2	9 Trifluoperazine t0/t2	10 tolbutamide t0/t2	11 Trifluoperazine t0/t2	12 DMSO t0/t2

Plate 2

Pooled Human Donor HepatoPac			Stromal Only Controls for Human HepatoPac - 3T3 J2 Mouse Fibroblasts		
13 DMSO t0/t2	14 Sunitinib t0/t2	15 Carbazeran t0/t2	16 Sunitinib t0/t2	17 Carbazeran t0/t2	18 DMSO t0/t2
13 DMSO t7	14 Sunitinib t7	15 Carbazeran t7	16 Sunitinib t7	17 Carbazeran t7	18 DMSO t7
19 DMSO t7	20 tolbutamide t7	21 Trifluoperazine t7	22 tolbutamide t7	23 Trifluoperazine t7	24 DMSO t7
19 DMSO t0/t2	20 tolbutamide t0/t2	21 Trifluoperazine t0/t2	22 tolbutamide t0/t2d	23 Trifluoperazine t0/t2	24 DMSO t0/t2

Plate 3

Rat HepatoPac					
37 DMSO t0/t2	38 Sunitinib t0/t2	39 Carbazeran t0/t2	40 Sunitinib t0/t2	41 Carbazeran t0/t2	42 DMSO t0/t2
37 DMSO t7	38 Sunitinib t7	39 Carbazeran t7	40 Sunitinib t7	41 Carbazeran t7	42 DMSO t7
43 DMSO t7	44 tolbutamide t7	45 Trifluoperazine t7	46 tolbutamide t7	47 Trifluoperazine t7	48 DMSO t7
43 DMSO t0/t2	44 tolbutamide t0/t2	45 Trifluoperazine t0/t2	46 tolbutamide t0/t2	47 Trifluoperazine t0/t2	48 DMSO t0/t2

Plate 4

Stromal Only Controls for Rat HepatoPac - 3T3 J2 Mouse Fibroblasts					
25 DMSO t0/t2	26 Sunitinib t0/t2	27 Carbazeran t0/t2	28 Sunitinib t0/t2	29 Carbazeran t0/t2	30 DMSO t0/t2
25 DMSO t7	26 Sunitinib t7	27 Carbazeran t7	28 Sunitinib t7	29 Carbazeran t7	30 DMSO t7
31 DMSO t7	32 tolbutamide t7	33 Trifluoperazine t7	34 tolbutamide t7	35 Trifluoperazine t7	36 DMSO t7
31 DMSO t0/t2	32 tolbutamide t0/t2	33 Trifluoperazine t0/t2	34 tolbutamide t0/t2	35 Trifluoperazine t0/t2	36 DMSO t0/t2

Plate 5 - matrix placement

<table>
<tr><td rowspan="2">3T3 J2 Mouse</td><td>Human Donor VNL HepatoPac</td><td>Pooled Human Donor HepatoPac</td><td rowspan="2">3T3 J2 Mouse</td></tr>
<tr><td colspan="2">Rat HepatoPac</td></tr>
</table>

Plate 5 - design for running experiment

Stromal Only	Human Donor VNL HepatoPac	Pooled Human Donor HepatoPac			Stromal Only
1 DMSO t0/t2	2 DMSO t0/t2	3 Quinidine t0/t2	4 DMSO t0/t2	5 Quinidine t0/t2	6 Quinidine t0/t2
1 DMSO t7	2 DMSO t7	3 Quinidine t7	4 DMSO t7	5 Quinidine t7	6 Quinidine t7
7 DMSO t7	8 DMSO t7	9 Quinidine t7	10 DMSO t7	11 Quinidine t7	12 Quinidine t7
7 DMSO t0/t2	8 DMSO t0/t2	3 Quinidine t0/t2	10 DMSO t0/t2d	11 Quinidine t0/t2	12 Quinidine t0/t2
400 uL Stromal Only Controls - 3T3 J2 Mouse Fibroblasts	**Rat HepatoPac 400 uL**		**Rat HepatoPac 300 uL**		**300 uL Stromal Only Controls - 3T3 J2 Mouse Fibroblasts**